Dear all,

The Annual Projects Conference in Biomedical Engineering is hosted by the Faculty of Biomedical Engineering at the Technion – Israel Institute of Technology. As the Dean of the Faculty of Biomedical Engineering and as the project course staff, we are pleased and honored to welcome you here.

The conference is hosting 4th year students who are eager to present their year-long projects and to receive feedback from academic researchers, industrial experts, and their peers. These projects implement the medical, engineering, and scientific tools that the students have acquired and developed during their BSc journey in Biomedical Engineering.

The students aim to provide solutions that meet research and development needs in the Biomedical industries and research departments. Through working on their projects, students gained invaluable, hands-on experience. They had to work through technical challenges and adhere to strict standards comparable to those in a real-world setting.
We believe that this hands-on experience engages graduates with the Biomedical industry and/or the wide variety of Biomedical research in a very strong way encouraging multidisciplinary work that is vital to the students' futures.

Additionally, we encourage the students to think out of the box to initiate new solutions and help foster their entrepreneurship skills. Above all, these projects are a key element of the faculty vision which strives to strengthen the long-term cooperation between academia and industry leaders.

In this booklet we are introducing the abstracts of all presented projects. We wish all students rewarding careers and bright futures. We hope that one day they will take an active part in similar projects as professional mentors from both the industry and academia.

Kindest Regards,
Prof. Shulamit Levenberg, Faculty Dean
Prof. Netanel Korin, Course Instructor

List of Abstracts

(1) Epileptic Seizures Prediction Based on ECG Signals Using Machine Learning Methods

Shlomi Shmuel[1,2], Galya Segal[1,2], Jacob Genizi[3], Moshe Hershkovitz[4], Joachim Behar[1], Noam Keidar[1,2], Yael Yaniv[1]
[1] Department of Biomedical Engineering, Technion - IIT, Haifa, Israel
[2] Faculty of Medicine, Technion IIT, Haifa, Israel
[3] Pediatric Neurology Unit, Bnai Zion Medical Center, Haifa, Israel
[4] Department of Neurology, Rambam Health Care Campus, Haifa, Israel

(2) Mother-Child Brain to brain Synchrony During Joint Story-Telling

Wurod Abu Elasal[1], Elia Khamesy[1], Joachim Behar[1], Michal Zivan[2], Tzipi Horowitz-Kraus[2]
[1] Faculty of Biomedical Engineering, Technion IIT, Israel
[2] Faculty of Education in Science and Technology, Technion IIT, Israel

(3) The Association Between Mother-Child Speech Synchrony During Dialogic Reading and Child's Cognitive Skills

Aseel Abdo[1], Maysaloon Baransi[1], Michal Zivan[2], Joachim Behar[1], and Tzipi Horowitz-Kraus[1,2]
[1] Department of Biomedical Engineering, Technion - IIT, Haifa, Israel
[2] Faculty of Education in Science and Technology, Technion - IIT, Haifa, Israel

(4) Atrial Blood Pressure Waveform Clustering

Ravid Ashash[1], Jonathan Horev[1], Joachim Behar[1], Danny Eytan[2]
[1] Biomedical Engineering Faculty, Technion - IIT, Haifa, Israel
[2] Pediatric Critical Care Unit, Rambam Health Care Campus, Haifa, Israel

(5) Big-Data Based Analysis of Sinoatrial Node Rejuvenation Attempts

Gal Shofel, Yonat Chen, Ori Shemla, and Yael Yaniv
Department of Biomedical Engineering, Technion - IIT, Haifa, Israel

(6) Biosensor for Detecting of Hematuria

Hadeel Abu Asaad, Dima Wakim, Joachim Behar, Natali Burger, Ramez Daniel
Department of Biomedical Engineering, Technion - IIT, Haifa, Israel

(7) Mood Tracking App for Cancer Patients Undergoing Immunotherapy

Adi Waisman, Rachelie Leber, Yosef Shamay
Department of Biomedical Engineering, Technion - IIT, Haifa, Israel

(8) Separation of Multiple Motor Memories through Implicit and Explicit Processes

Yuval Shaine, Gefen Dawidowicz, Firas Mawase
Department of Biomedical Engineering, Technion – IIT, Haifa, Israel

(9) ECoG-based Intraoperative Functional Mapping of the Cerebral Cortex During Awake Craniotomies

Taima Zoabi[1], Leen Ileimi[1], Anat Grinfeld[1], Shaked Ron[2], Omer Zarchi[3], Firas Mawase[1]
[1] Faculty of Biomedical Engineering, Technion - IIT, Haifa, Israel
[2] Faculty of Medicine, Technion - IIT, Haifa, Israel
[3] Intraoperative Neurophysiological Service, Rabin Medical Center, Israel

(10) An MRI Compatible 3D Printed Split-belt Treadmill for Motor Neuroscience Research

Tania Assaf [1], Wajdi Nicola[1], Ameer Lawen[2], Itamar Kahn[2], Anat Grinfeld[1], Firas Mawase[1]
[1] Faculty of Biomedical Engineering, Technion IIT
[2] Faculty of Medicine, Technion IIT

(11) Reorganization of Functional Networks Following MRI-guided Focused Ultrasound Treatment in Essential Tremor Patients

Daniel Olshvang[1], Or Motzary[1], Firas Mawase[1], Anat Grinfeld[1,2], Gil Zur[2], Noam Bosak[3], Itamar Kahn[4]
[1] Faculty of Biomedical Engineering, Technion IIT
[2] Department of Radiology, Rambam Health Care Campus
[3] Department of Neurology, Rambam Health Care Campus
[4] Faculty of Medicine, Technion IIT

(12) Identification and Quantification of Synapses from Images of Expanded Brains

Tali Marchevsky[1], Sapir Noah[1], Anat Grinfeld[2], Limor Freifeld[3]
[1] Department of Biomedical Engineering, Technion - IIT, Haifa, Israel
[2] Neuro-Engineering laboratory, Technion IIT

(13) Quantitative DW-MRI analysis algorithms

Judit Ben Ami[1], Marina Khizgilov[1], Anat Grinfeld[2], Moti Freiman[1]
[1] Department of Biomedical Engineering, Technion - IIT, Haifa, Israel
[2] Department of Medical Imaging, Rambam Health Care Campus, Haifa, Israel

(14) Visualization Software for Pediatric Crohn's Disease Assessment by Multi Planar Reformation

Yael Zaffrani[1], Anat Ilivitzki[2], Anat Grinfeld[1], and Moti Freiman[1]
[1] Department of Biomedical Engineering, Technion - IIT, Haifa, Israel
[2] Radiology Unit, Ruth Rappaport Children's Hospital, Haifa, Israel

(15) Develop of Diagnostic System for Preventing Sudden Cardiac Death among Athletes

Matti Zeev[1,2], Nimrod Baram[1], Ido Weiser Bitoun[1,2], Alexandra Alexandrovic[1], Michal Zivan[1], Yeal Yaniv[1]
[1] Faculty of Biomedical Engineering, Technion - IIT, Haifa, Israel
[2] Faculty of Medicine, Technion - IIT, Haifa, Israel

(16) Detecting heart abnormalities using a novel platform of digitized 12-lead ECG

Nitzan Avidan[1], May Buzaglo[1], Vadim Gliner[2], Yael Yaniv[1]
[1] Biomedical Engineering Faculty, Technion - IIT, Haifa, Israel
[2] Computer Science Faculty, Technion - IIT, Haifa, Israel

(17) Development of a Non-Invasive Clinical Tool for Analyzing SAN & ANS Function and Identifying Cardiac Pathologies

Opal Nimni, Ayelet Lotan, Ido Weiser-Bitoun, Yael Yaniv
Faculty of Biomedical Engineering, Technion – IIT, Haifa, Israel

(18) MRI Brain Tumor Segmentation

Shany Biton, Zohar Avinoam, Anat Grinfeld, Moti Freiman
Biomedical Engineering Faculty, Technion - IIT, Haifa, Israel

(19) Brain Tumor MRI Image Segmentation

Michaela Ayoun, Moti Freiman, Anat Grinfeld
Biomedical Engineering Faculty, Technion - IIT, Haifa, Israel

(20) Feasibility of Ultrasonic Thermal Monitoring Using Coded Excitations for Focused Ultrasound Hyperthermia

Noy Parti, Tomer Romano, Daniel Dahis, Haim Azhari
Department of Biomedical Engineering, Technion - IIT, Haifa, Israel

(21) Disease diagnosis based on Bio markers Using tagged proteins transport through Nano-Pore system and Machine learning

Maya Eytani, Oren Shorr, Michal Zivan, Shilo Ohayon, Amit Meller
Faculty of Biomedical Engineering, Technion IIT

(22) Laser Speckle Contrast Imaging in Biomedical Optics

Arseny Belousov[1], Dmitry Rudman[1], Yokhay Dan[2], Michal Zivan[1], Rami Shinnawi[2]
[1] Biomedical Engineering Faculty, Technion - IIT, Haifa, Israel
[2] AntiShock (MindUP), Haifa, Israel

(23) Compact spectrally encoded interferometry probe for imaging acoustic vibrations in the tympanic membrane

Lidan Fridman, Matan Hamra, Rotem Yacoby and Dvir Yelin
Biomedical Engineering Faculty, Technion - IIT, Haifa, Israel

(24) A Low-Cost 3D Printed Prosthetic Hand for Transhumeral Amputations

Niv Rebhun[1], Sofia Rozenberg[1], Yair Herbst [2], Oscar Lichtenstein [1], Yoav Medan[3]
[1] Biomedical Engineering Faculty, Technion - IIT, Haifa, Israel
[2] Department of Mechanical Engineering, Technion - IIT, Haifa, Israel
[3] Haifa3D Co-Founder and Chairman, Visiting Scientist, Technion - IIT, Haifa, Israel

(25) A Modular, Task Specific End Effector for A Low-Cost 3d Printed Prosthetic Hand

Ayala Goldstein[1], Yair Herbst[2], Oscar Lichtenstein[1], Yoav Medan[1]
[1] Department of Biomedical Engineering, Technion - IIT, Haifa, Israel
[2] Faculty of Mechanical Engineering, Technion – IIT, Haifa, Israel

(26) Fully Automatic Adjustable CAD Model of a Wrist Powered, Low- cost, 3D Printed Prosthetic Hand

Mark Kels[1], Yair Herbst[2,3], Oscar Lichtenstein[1], Yoav Medan[3]
[1] Department of Biomedical Engineering, Technion - IIT, Haifa, Israel
[2] Faculty of Mechanical Engineering, Technion – IIT, Haifa, Israel
[3] Haifa3D, Haifa, Israel.

(27) Effect of Drag Reducing Polymers (DRPs) on Recirculation and the Deposition of Targeted Nano-Carrier in Human Arterial Models

Neta Tuaf, Oscar Lichtenstein, Maria Khoury, Netanel Korin
Department of Biomedical Engineering, Technion - IIT, Haifa, Israel

(28) Clot Fibrinolysis in CRAO Models Using Thrombolytic Therapy Triggered by Externally Low Intensity Ultrasound

Or Mizrahi, Omer Gottlieb, Moran Levi, and Netanel Korin
Department of Biomedical Engineering, Technion – IIT, Haifa, Israel

(29) Remote Speech Therapy technology

Marina Tulchinsky[1], Roni Keshet[1], Ori Shahar[1], Shaked Ron[2], Oscar Lichtenstein[1]
[1]Department of Biomedical Engineering, Technion - IIT, Haifa, Israel
[2]Department of Medicine, Technion - IIT, Haifa, Israel

(30) Optimization of Dual Drug Co-Encapsulation in Cancer Targeted Nanoparticles

Amjad Marie, Sanaa Dallashi, Dana Azagury, Arbel Artzy-Schnirman, Yosi Shamay
Department of Biomedical Engineering, Technion- IIT, Haifa, Israel

(31) Increased Extracellular Vesicle (EV) Production From 3D Engineered Skeletal Muscle Tissue Under Mechanical Stretching

Tahel Carmon, Adina Israel Fried, Lior Debbi, Shaowei Guo, Arbel Artzy-Schnirman, Shulamit Levenberg
Biomedical Engineering Faculty, Technion IIT

(32) The effects of natural remedies on the invasiveness of metastatic cancer cells

Stav Elkabetz, Sally Kortam, Arbel Artzy-Schnirman and Daphne Weihs
Department of Biomedical Engineering, Technion - IIT, Haifa, Israel

(33) Developing an Optimized Method for Efficient Automated Nano- Particles Preparation and Characterization

Yarden Roth, Maytal Avrashami, Yuval Harris, Arbel Artzi-Shnirman, Yosi Shamay
Department of Biomedical Engineering, Technion - IIT, Haifa, Israel

(34) Wearable Diagnostic Patch for Monitoring Health Status

Nadi Hathot[1], Jalil Bishara[1], Youbin Zheng[2], Arbel Arzy-Schnirman[1], Hossam Haick[2]
[1]Faculty of Biomedical Engineering, Technion IIT
[2]Faculty of Chemical Engineering, Technion IIT

(35) Effects of Cancer Conditioned Medium of High Metastatic Cells on The Invasive Behaviour of low-Metastatic Pancreatic Cancer Cells

Liubov Akselrod, Yulia Merkher, Sally Kortam, Daphne Weihs
Faculty of Biomedical Engineering, Technion IIT

(36) Recombinant p27 Liposomal Drug Intended to Inhibit the Uncontrolled Proliferation of Cancerous Cells

Maya Hershko[1,3], Danielle Sitry Shevah[3], Arbel Artzy Schnirman[1], Avi Schroder[1,2]
[1] Faculty of Biomedical Engineering, Technion IIT
[2] Faculty of Chemical Engineering, Technion IIT
[3] Faculty of Medicine, Technion IIT

(1)

Epileptic Seizures Prediction Based on ECG Signals Using Machine Learning Methods

Shlomi Shmuel[1,2], Galya Segal[1,2], Jacob Genizi[3], Moshe Hershkovitz[4], Joachim Behar[1], Noam Keidar[1,2], Yael Yaniv[1]

[1] Department of Biomedical Engineering, Technion - IIT, Haifa, Israel
[2] Faculty of Medicine, Technion IIT, Haifa, Israel
[3] Pediatric Neurology Unit, Bnai Zion Medical Center, Haifa, Israel
[4] Department of Neurology, Rambam Health Care Campus, Haifa, Israel

Introduction: It is estimated that around 50 million people suffer from epilepsy worldwide. A person diagnosed with epilepsy suffers from neurobiological, cognitive, psychological, and social consequences of this disease. One of the most disabling aspects of epileptic seizures is attributed to their apparently sudden, unexpected nature in which their strike, and therefore may lead to serious injuries. Apart from physical harm, patients who fail to achieve complete seizure balance often feel intensively helpless, with their daily lives being strongly affected. Currently there is no clinical tool to predict epileptic seizure.

Methods: We collected long-term ECG recordings from patients diagnosed with epilepsy from a large medical center in Israel (n=24) and from university of Siena, Italy (n=15). We preprocessed the biological signal and applied heart rate variability (HRV) analysis to reveal changing patterns in the cardiac activity, alluding autonomic activity preceding an upcoming seizure.

We designed a predictive model based on temporal convolutional networks (TCN), a state-of-the art deep learning algorithm. This model has two main qualities which make it especially suitable for predictive tasks: (1) its ability to use long term history of a signal, and (2) causality, meaning the decision to raise an alarm is based exclusively on the past. Our model was designed to give an alarm in the interval of 1-15 minutes before a seizure onset. The ECG database was divided into train, validation, and test sets. The validation set was used for optimization of the model parameters, and the test set was used for evaluation of the model performance.

Results: Each record in the test set was divided into 15-minute intervals, each interval was binary classified as a success (true positive or true negative) or as a failure (false positive or false negative). Overall performance was calculated on Siena database using leave-one-out cross validation, and summarized in the Table 1:

specificity	sensitivity
94.2%	24.1%

Table 1: Model performance

Conclusions:

Previous works have showed that ECG-based seizure prediction is possible if patient-specific analysis is made. In this work we used ECG recordings captured by varying measurement equipment from different countries and showed a more generalized system performances based on heart rate variability. We demonstrated a high level of specificity and believe that using larger number of patients and relying also on EEG recordings may even further improve our results.

Keywords: Epilepsy; Prediction; Heart Rate Variability; Deep Learning; Temporal Convolutional Networks.

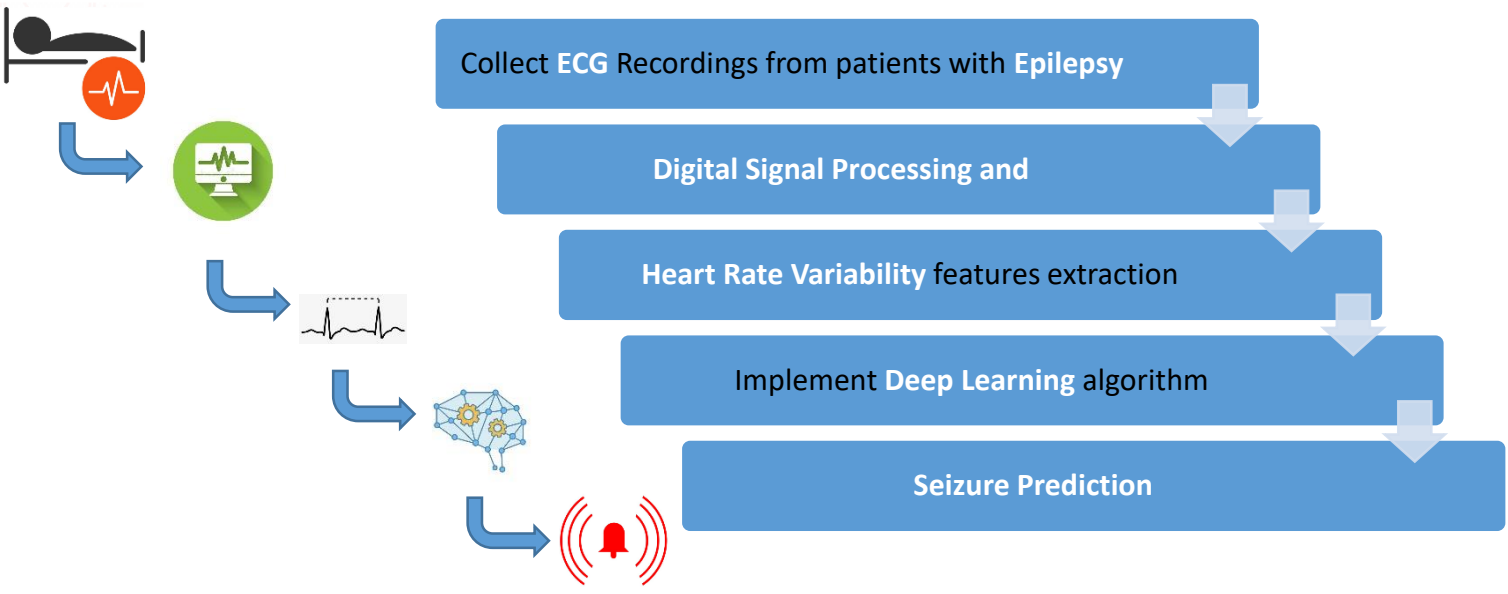

Figure 1: Main blocks of our work

(2)

Mother-Child Brain to brain Synchrony During Joint Story-Telling

Wurod Abu Elasal[1], Elia Khamesy[1], Joachim Behar[1], Michal Zivan[2], Tzipi Horowitz-Kraus[2]

[1] Faculty of Biomedical Engineering, Technion IIT, Israel
[2] Faculty of Education in Science and Technology, Technion IIT, Israel

Introduction: The developing brain is affected by genes and the environment surrounding them specifically interactions with their parents. Exploring parent-child synchrony during shared interactions and its association with child's cognitive and social development, can deepen our understanding regarding parent-child quality of interaction and how it relates to child's brain development along lifespan. Brain-to-brain synchrony (hyper-scanning) in parents and children is a new and growing research field enabling a detection of mutual, synched brain activation of two individuals. Parent-child mutual engagement during a shared dyad is related to increased neural synchrony. Parent-child joint storytelling, which is a form of interpersonal interaction, is known to promote young children's linguistic and emotional skills. The study of parent-child brain-to-brain synchrony during joint storytelling, particularly in the Arabic language, has not been reported yet and can provide quantifiable measurements regarding the quality of interaction and how these are related to the child's cognitive skills.

Methods: Native Arabic speaking pairs of participants (n=10) were recruited (child mean age= 5.03 , SD=1.19; parents mean age=33.40, SD=4.30). Children underwent 7 verbal and non-verbal cognitive tests. The tests were taken before and after a storytelling intervention period of 4 weeks, which included a total of 20 story-telling sessions. In addition, six parent-child pairs underwent EEG hyper-scanning (using EMOTIV EPOC 14 channels, 128Hz sampling rate) following the intervention. During the EEG session the following conditions were applied: a)Formal Arabic language storytelling, b)colloquial (the spoken language) storytelling, c)resting state, d)formal story-telling with phone distracting the mother, e)separate activities for mother and child

EEG signals preprocessing phase included removing DC offset by applying 0.16Hz high-pass filter and manual noise filtering. In order to quantify the level of synchrony in each parent-child pair of electrodes for each condition, we used circular correlation (CCor) using MATLAB circular statistics toolbox. Non-parametric bootstrap-based t-tests were used to analyze the differences in interbrain synchronization between each

two tested conditions. The p values were corrected using FDR-correction for multiple comparisons.

Results: Higher mother-child brain to brain synchrony was observed in the joint-storytelling conditions compared to non-interaction conditions. Specifically, higher synchrony was observed in both formal and colloquial storytelling in comparison to resting state, separate activities, and interrupted storytelling. Higher brain-to-brain synchrony was observed in the colloquial (spoken language) vs. the formal written storytelling. The increase in brain-to-brain synchrony was mainly observed in the between the mothers left hemisphere with the child's right hemisphere. In addition, all children showed improvement in cognitive verbal and nonverbal skills post the intervention period.

Conclusions: Parent-child joint storytelling is associated with increased inter brain synchronization in comparison to non-shared activities and interrupted activities. The increase was mainly observed between language production regions of the mother and language comprehension and emotional brain regions of the child. In addition, greater synchronization was observed for the colloquial (spoken language) storytelling vs the formal written storytelling emphasizing the challenges in diglossia in Arabic. Shared activities, such as storytelling between mother and child improve the child's cognitive skills.

Keywords: Brainwaves correlation, cognitive skills, hyper-scanning, interpersonal shared activities.

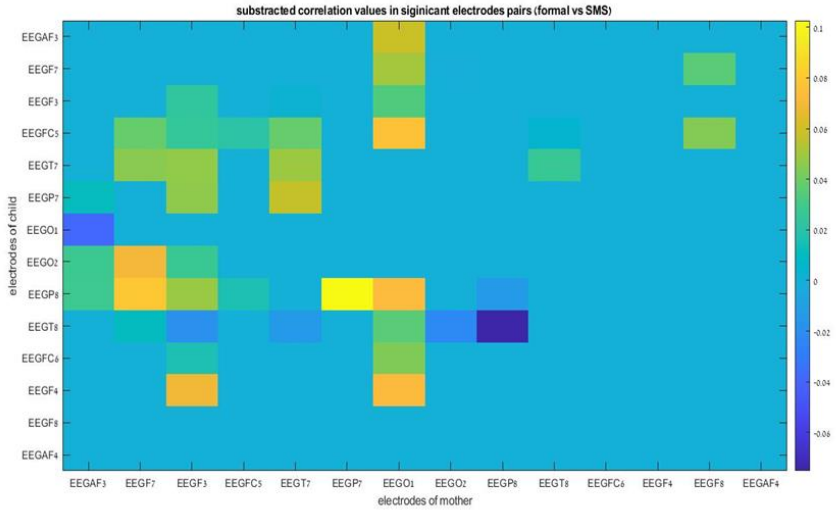

Figure 1: Positive values, displayed in yellowish color, represent distinct brainwaves synchrony for the formal storytelling, whilst negative values, displayed in deep blue colors, represent distinct brain waves synchrony for the interrupted condition. greater brain to brain correlation is observed in the formal storytelling in comparison to the interrupted one.

(3)

The Association Between Mother-Child Speech Synchrony During Dialogic Reading and Child's Cognitive Skills

Aseel Abdo[1], Maysaloon Baransi[1], Michal Zivan[2], Joachim Behar[1], and Tzipi Horowitz-Kraus[1,2]

[1] Department of Biomedical Engineering, Technion - IIT, Haifa, Israel
[2] Faculty of Education in Science and Technology, Technion - IIT, Haifa, Israel

Introduction: Parent-child interaction is a research topic that has been extensively studied in developmental psychology, but the effect of parent-child interaction on physiological synchrony is further to be studied. Parent-child synchrony level represents the quality of interaction by providing a quantitative and continuous description of the interaction. Previous studies have shown that parent-child behavioral synchrony from infancy effects the child's cognitive development. Dialogic reading (DR), a method guiding a dialogue with the child during storytelling while asking questions about the text, was found to be related to a better acquisition of language and attention skills among children. However, it is still unknown if a parent-child speech synchrony exists during a DR interaction, and whether the level of synchrony is related to better child cognitive skills following a DR intervention. The present study aims to answer these questions.

Methods: The project was conducted on 10 pairs of Arabic speaking mothers (mean age= 33.4 years) and their children (4-7 years old). The procedure included performing a DR intervention at home during which parents read stories dialogically to their children for 5 days a week for 4 weeks (overall of 20 sessions). A set of behavioral tests were conducted before and after intervention. All DR sessions were audio recorded with the parents' cellular phones. The data analysis included a separation of the mother and child voices using MATLAB and WavePad software, extracting the speech properties (Pitch, Intensity, Speech Rate, Number of syllables) of the mother and the child using Praat software. Finally, a statistical analysis was preformed to study the relationship between the mothers' and children speech properties during the DR dyads in relations to the child's cognitive skills improvement following the intervention period.

Results: For each pair of participants, 4 linear regressions were preformed, one for each speech parameter, over all DR sessions, to evaluate the level of speech synchrony between the mother and child. Results showed that four pairs of participants had significant relations between mother and child for all 4 speech parameters ($p<0.05$). Two pairs of participants had significant relations for 3 speech parameters ($p<0.04$). Two pairs of participants had significant relations for 2 speech parameters ($p<0.005$) and 2 pairs of participants had significant relations for 1 speech parameter ($p<0.02$). In addition, the children showed improvement in all cognitive tests following the

intervention ($p<0.05$). Moreover, among mother-child pairs (n=6) that exhibit higher speech synchrony (at least for 3 out of 4 speech parameters), the children showed higher trends of cognitive skills improvement than the children in mother-child pairs with a lower speech synchrony.

Conclusions: In the present study, we aimed to create a tool defining the level of speech synchronization during a mother-child DR interaction, and its effect on child's cognitive skills. Our findings show high levels of speech synchrony accounting for different speech parameters during the DR interaction. In addition, better improvement of the behavioral tests following the intervention period was observed among mother-child pairs who had a higher speech synchrony. These results suggest that better mother-child speech synchrony supports the child's cognitive skills.

Keywords: Dialogic reading, Parent-child interaction, Speech analysis, Synchrony.

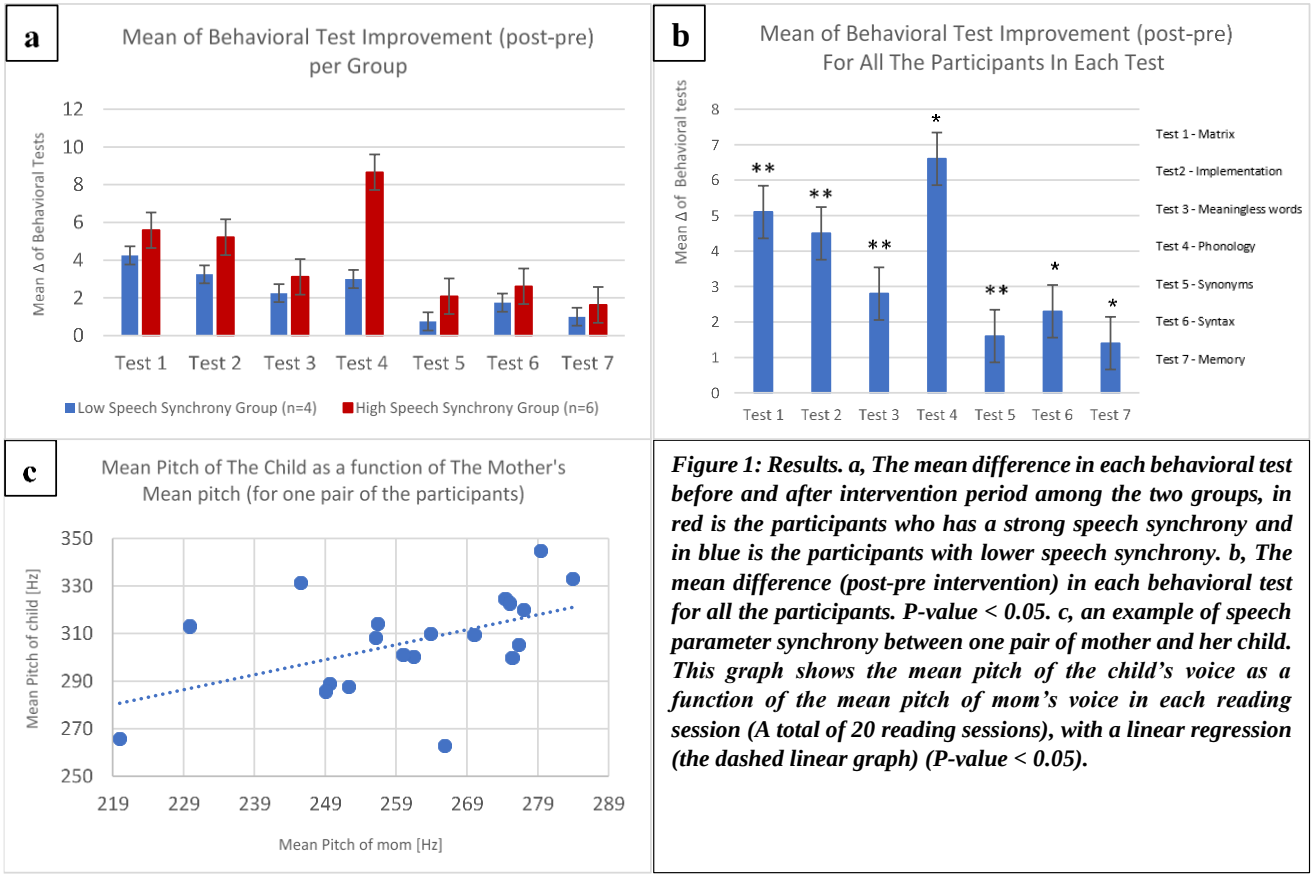

Figure 1: Results. a, The mean difference in each behavioral test before and after intervention period among the two groups, in red is the participants who has a strong speech synchrony and in blue is the participants with lower speech synchrony. b, The mean difference (post-pre intervention) in each behavioral test for all the participants. P-value < 0.05. c, an example of speech parameter synchrony between one pair of mother and her child. This graph shows the mean pitch of the child's voice as a function of the mean pitch of mom's voice in each reading session (A total of 20 reading sessions), with a linear regression (the dashed linear graph) (P-value < 0.05).

(4)

Atrial Blood Pressure Waveform Clustering

Ravid Ashash[1], Jonathan Horev[1], Joachim Behar[1], Danny Eytan[2]

[1] Biomedical Engineering Faculty, Technion - IIT, Haifa, Israel
[2] Pediatric Critical Care Unit, Rambam Health Care Campus, Haifa, Israel

Introduction: Patients in the intensive care unit (ICU) are being strictly monitored. Physiological signals as electrocardiogram (ECG), atrial blood pressure (ABP), central venous blood pressure (CVP) etc., are being recorded continuously throughout the hospitalization period. These signals contain significant information about the patient's physiological condition and about the functionality of the different body systems. The ABP has an important role in the patient's prognosis. For example: low ABP may indicate a myocardial infraction, sepsis or bleeding from the gastrointestinal tract.

Our goal is to find unique patterns in the blood pressure waveform which repeat themselves in the signal several times. We hope to derive from these patterns richer insights about the patient's clinical condition.

Methods: Our data is 62 ABP recordings from children in the ICU of Rambam hospital, which had a cardiac arrest during their hospitalization period. The average length of the recordings is 3 hours, 1.5 hours before and after the cardiac arrest. As part of the preprocessing, we implemented a third order bessel low pass filter with cutoff frequency of 25 Hz. Moreover, we manually removed noisy and non-physiological segments from the signals. We segmented the signals into windows which are 5 minutes length with 2 minutes overlapping. From each window we extracted features while focusing on features with cardiovascular importance such as: average systolic/diastolic pressure, average length of systolic/diastolic phase, mean spectral power etc. In total we extracted 51 features from each window. We used 2 different algorithms for the window's clustering: k-means clustering and t-distributed_stochastic neighbor embedding (t-SNE). In order to evaluate the number of ideal clusters in the data we used Calinski-Harabasz and Davies–Bouldin indexes. Afterwards we clustered the data into 6 clusters with the t-SNE algorithm. To evaluate the cardiovascular meaning of each cluster we examined the 10 nearest windows to each cluster's centroid in the time domain. Further, we examined the distribution of each feature among the different clusters.

Results:

Cluster no.	Number of windows in a cluster
1	241 (5.93%)
2	1056 (25.5%)
3	2152 (52.5%)
4	1 (0.02%)
5	3 (0.05%)
6	628 (16%)

Table 1: The distribution of windows among the clusters.

Conclusions: At the moment, it is difficult for us to say whether the different clusters have cardiovascular significance. Clusters 4 and 5 are very small and this raises questions about the quality of the results. To obtain a more thorough understanding of the results, it is necessary to check for every cluster the following datum: from which patient and during what time in the recordings, the windows that belong to that specific cluster came from. We hope that this kind of data will help us to get a better grasp of the results.

Keywords: Atrial Blood pressure; K-means; t-SNE.

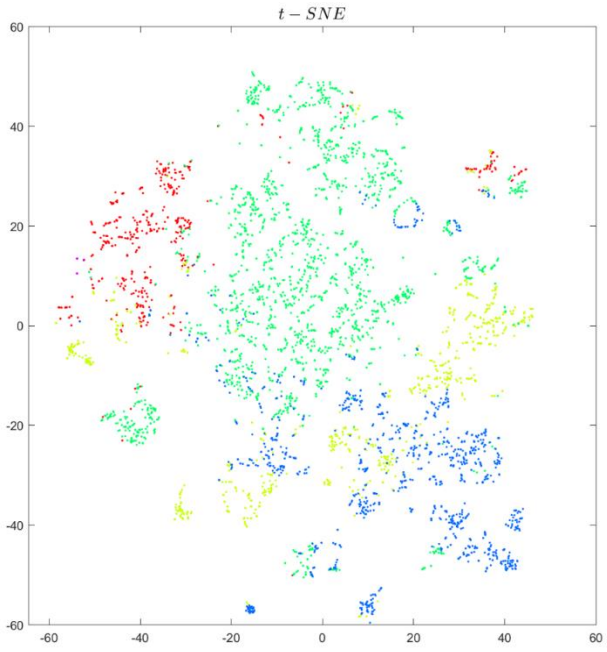

Figure 1: The different clusters using t-SNE

(5)

Big-Data Based Analysis of Sinoatrial Node Rejuvenation Attempts

Gal Shofel, Yonat Chen, Ori Shemla, and Yael Yaniv

Department of Biomedical Engineering, Technion - IIT, Haifa, Israel

Introduction: Heart disease have been one of the leading causes of death in recent decades in the United States and are significantly more common among the elderly population. While life expectancy worldwide is constantly rising, the number of elderly people with cardiovascular disease is expected to rise as well. Understanding the mechanisms of heart disease and the aging effect on them is crucial for better healthcare and improved quality of life in the future. Research in mice showed that the function of the sinoatrial node (SAN) decreases with age due to changes in electrical conduction and changes in the intra-cellular mechanisms of action potential. These findings are accordant with research preformed on human SAN tissue. Therefore, by studying electrogram (EGM) recordings of SAN, it is possible to understand the effect of age on SAN function and even find appropriate treatment for its decline in function. Since SAN is one of the key factors to determine the heart rate and rhythm, research in the field of aging processes on pacemaker tissue (ex-vivo) is necessary

Methods: EGM recordings of young mice (n=18) and old mice (n=20) from electrophysiology lab's databases were analyzed using PhysioZoo. Using MATLAB's digital signal processing tools, a toolbox of 91 features which measure the morphology of the EGM was designed. All the features were then divided into 14 groups with similar characteristics and the most reliable features were selected using a dedicated algorithm. EGM recordings of old mice with IBMX at 1, 10, 20 and 100 µM (n=29) from previously published work were analyzed using PhysioZoo and compared each with the 2 groups without the intervention. For each of the selected features, the tool determines whether the intervention was beneficial (the experimental group measurements were closer to the results of the young mice than to the adults), caused eccentric change (the experimental group measurements became more extreme than the young mouse group measurements), caused unwanted side effects (Experiments of the experimental group became more extreme than those of the adult group of mice).

Results: In the case of IBMX at a dose of 100 µM we found that the dosage wasn't beneficial.

Conclusions: The purposed method makes it possible to conduct studies of the effectiveness of various medicines through digital signals analysis, and reach conclusions conveniently and efficiently. It saves time for researchers by finding the

most relevant features for their experiment and allows them to compare several experimental groups simultaneously. Furthermore, the purposed method makes it possible to analyze a variety of cyclic biological signals. For EGMs, the efficiency of medicine can be measured using morphological parameters. Additional methods of intervention should be tested at different concentrations to reach conclusions about the effectiveness of the medicines.

Keywords: Sinoatrial Node (SAN), Electrogram (EGM), Big Data, Features Selection.

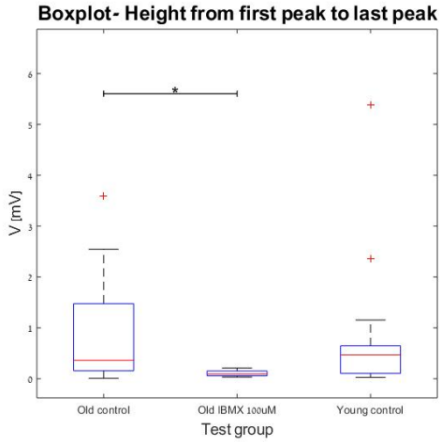

Figure 1: comparison between 2 groups without the intervention and a treated group according the feature "Height from first peat to last peak"

(6)

Biosensor for Detecting of Hematuria

Hadeel Abu Asaad, Dima Wakim, Joachim Behar, Natali Burger, Ramez Daniel

Department of Biomedical Engineering, Technion - IIT, Haifa, Israel

Introduction: Hematuria is a very critical symptom that can be a signal to serious problems in the urinary tract or the kidneys. In this research we create an easy, reliable and rapid biosensor for heme molecules detection in the urine. Whole cell biosensors have proved to be very useful in detecting biological biomarkers and molecules and enables real-time data analysis. However, for whole cell biosensors there are several limitations that might make them unreliable in different medias and have a low ON-OFF ratio.

Method: We present an environmentally resilient biosensor based on genetically engineered *Escherichia coli (E. coli)*. Which can generate light energy when it detects heme molecule. This light energy is then transferred to an electrical sensor that is capable of detecting low level light and transferring the information to a portable device. In this work we demonstrate that the biosensor built can be reliable even in complex medias, such as the urine, giving us a high Signal to Noise ratio and reliable results. Furthermore, we built a theoretical model that excellently matched the measured bacterial light signal. This is supported by experimental results of the light energy signal that is measured using a FACS and plate reader in addition to the electrical sensor.

Results: The results shown in Figure 1a .and 1b. are taken from the integrational experiment, where the urine, our designed bacteria and the heme molecules would flow through the microfluidic chamber and the electrical sensor will detect the light generated from the culture. The sensor used in the final experiment measures the photons resulted from our genetically modified bacteria or Biosensor. The graph in Figure1. Shows that there is almost no change in the photon detection frequency with no hemin added. while in Figure 2. The graph shows an increase of photon detection frequency with varying concentrations of heme molecules in the urine.

Conclusions: These next-generation whole cell biosensors with improved computing and amplification capacity could meet clinical requirements and should enable new approaches for medical diagnosis. In addition, those results indicate the way forward for future work, highlighting the improvements required for clinical-level accuracy, which could allow for detecting many more molecules in the urinary tract and help in early diagnosis of diseases.

Keywords: Biosensor, Hematuria, Heme, diagnosis, Biomarkers, Genetic engineering, FACS, Plate Reader, NO-OFF ratio, LB

a.

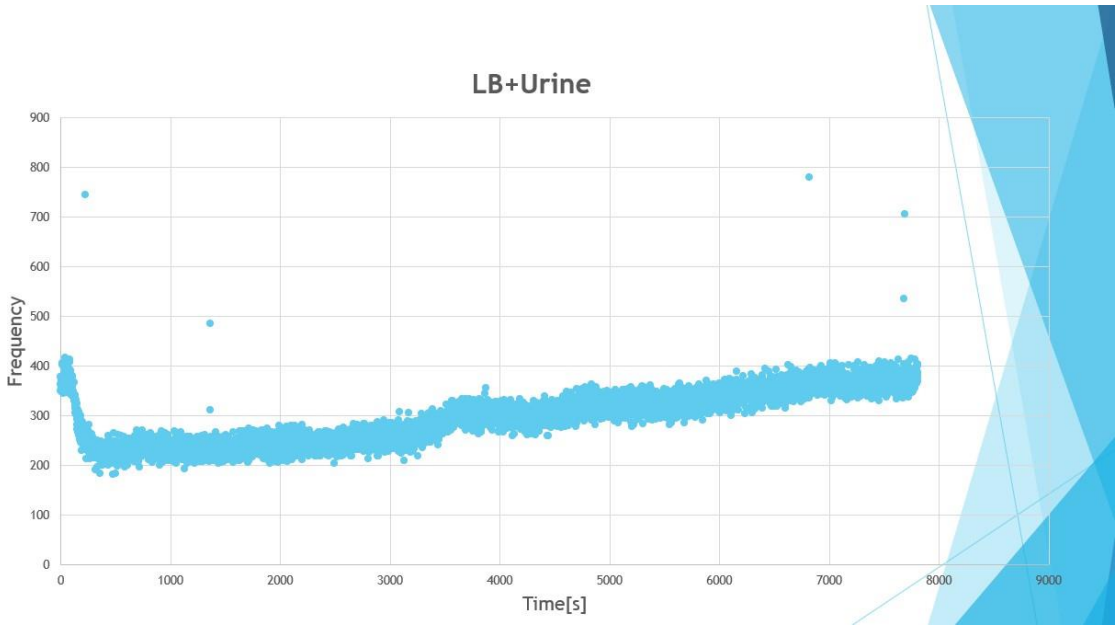

b.

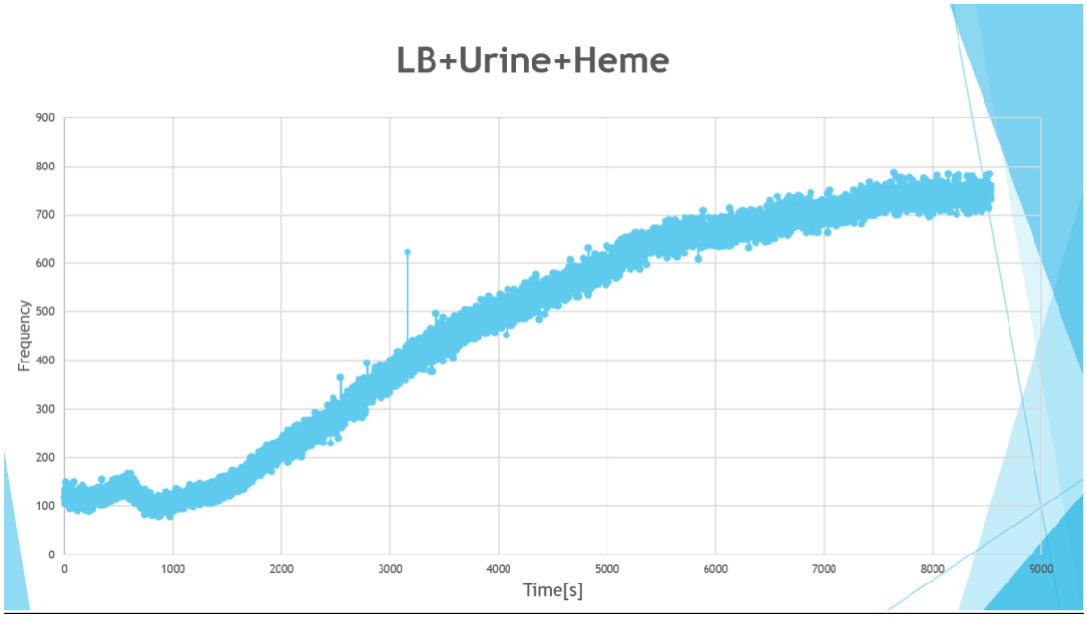

Figure 1: (a) Frequency of photon detection with urine and LB, (b) Figure 2. Frequency of photon detection with 20 µl of heme molecules added to the urine and the LB.

(7)

Mood Tracking App for Cancer Patients Undergoing Immunotherapy

Adi Waisman, Rachelie Leber, Yosef Shamay

Department of Biomedical Engineering, Technion - IIT, Haifa, Israel

Introduction: Immunotherapy is a type of treatment in which the activity of the immune system is manipulated in order to fight diseases such as cancer. Immunotherapy is gaining popularity as a treatment for melanoma and non-small cells lung cancer. While immunotherapy has shown outstanding response in small patient population of several cancer types, most patients still do not response to these new therapies. Evidence are accumulating that the mental and psychological state of patients can affect the function of the immune system and therefore may affect the response to immunotherapy. Discovering such connection may improve response by adopting holistic treatment plans, caring for both the mental and physical health of patients, however current methods for tracking patients' mental wellbeing in a clinical trial environment are cumbersome and do not allow for continuous monitoring.

Methods: A hybrid, light and easy to use mobile application was designed, compatible with most smartphones and smart devices, using JavaScript, React.js and React Native frameworks. Emoji based mood report was adopted for simplicity and ease of use. An authentication mechanism and a real-time database were implemented using Firebase, granting a blinded experiment with simple data collection, all while keeping patients' privacy. The app was translated to four languages to meet requirements for a clinical trial setting.

Results: Preliminary data collection merely began, yet initial data shows promise that an emoji-based mood reporting is an effective approach to distinguish healthy population from ill population.

Conclusions: Sufficient amounts of data are required; therefore, data collection continues. Adding more features to the app can give a more whole picture of patients' wellbeing and its effects on immunotherapy.

Keywords: Immunotherapy; Cancer; App; Mental Health.

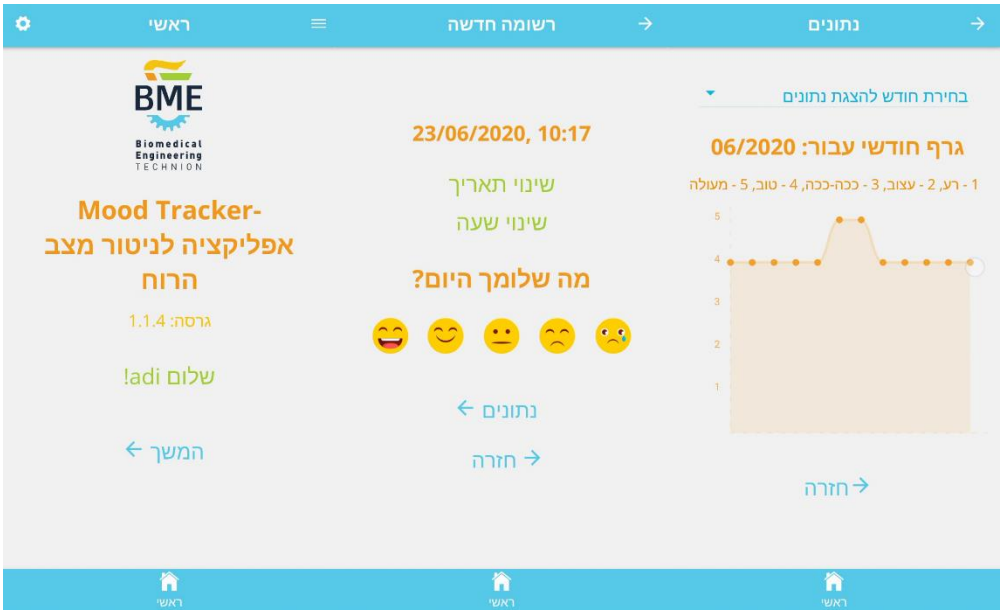

Figure 1: App welcome page, mood report page and monthly chart page.

(8)

Separation of Multiple Motor Memories through Implicit and Explicit Processes

Yuval Shaine, Gefen Dawidowicz, Firas Mawase

Department of Biomedical Engineering, Technion – IIT, Haifa, Israel

Introduction: The ability to learn new motor skills without interfering with old ones is important for acquiring and maintaining a broad motor repertoire. Formation of the motor memory is believed to transpire through small corrections after each learning trial. This learning process is comprised of multiple distinct components, at least one of which is implicit, slow and sensitive to sensory prediction error, and another which is explicit, fast and strategy-based. However, if the adjustments made to the memory during learning cancel out, interference occurs and the learning process is incomplete. This is what typically happens when direction of perturbation switches randomly from trial to trial. In this case, the opposing learning directions interfere and neither perturbation is learned. This interference, however, can be markedly reduced when appropriate contextual cues, like associating each perturbation with a unique subsequent follow-through movement (Howard et al., 2015; Sheahan et al., 2016), can segregate learning of the opposing perturbation into distinct motor memories. Nevertheless, the contribution of the implicit and explicit processes that underlie separation of motor memories remains unclear.

Methods: We designed reaching experiments and manipulated the implicit and explicit components while participants learned opposing visuomotor perturbations (clockwise or counter-clockwise) that were randomly selected for each trial with a second unperturbed follow-through movement. First, we isolated the *implicit component* by introducing error-clamp trials that minimize the use of explicit strategy: while moving to the central target, the cursor showed a fixed trajectory of 10° from the central path and at an opposite direction to the follow through target. The participants were instructed to continue aiming for the central target and to ignore the cursor manipulation. Second, we isolated the *explicit component* by using a delayed movement-based feedback that minimize the use of implicit component. At the end of the full movement participants were instructed to remain at the terminal position of the movement until the feedback was displayed, this appeared after a 2 sec delay. the feedback indicated the position of the cursor where the hand crossed the first target. The participants were instructed to try and fix the manipulation.

Results: Participants in both explicit (n=13) and implicit groups (n=12) were able to differentiate between the opposite directions and learn the opposing movements. Over

the course of adaptation, participants successfully compensated for the error and were able to reduce interference between opposing perturbations.

Conclusions: Our results show that the ability to separate two motor memories that normally interfere depends on both implicit and explicit processes.

Keywords: motor learning, follow-through movement, implicit and explicit processes

(9)

ECoG-based Intraoperative Functional Mapping of the Cerebral Cortex During Awake Craniotomies

Taima Zoabi[1], Leen Ileimi[1], Anat Grinfeld[1], Shaked Ron[2], Omer Zarchi[3], Firas Mawase[1]

[1] Faculty of Biomedical Engineering, Technion - IIT, Haifa, Israel
[2] Faculty of Medicine, Technion - IIT, Haifa, Israel
[3] Intraoperative Neurophysiological Service, Rabin Medical Center, Israel

Introduction: Awake craniotomy is a complicated neurosurgical operation. It is mainly performed in cases of severe epilepsy or brain tumors that are close to cerebral cortices involved in motor and language functions. To maximize lesion resection while minimizing post-surgery neurological deficits, the cerebral cortex is being mapped according to functionalities. For the past decade, the gold standard method for intraoperative cortical mapping has been the Electrical Cortical Stimulation (ECS). In ECS, a weak electrical current is directly delivered to the awake patient's cortex, eliciting or inhibiting motor and linguistic responses which are observed. An emerging method for intraoperative mapping utilizes the subdural electrocorticography (ECoG). The functional map based on the recordings of ECoG and the event-related power spectral changes could potentially avoid some of the ECS drawbacks and thus provide a safer and faster procedure. This being said, the initial set-up of a closed-loop decision support system, aiming to synchronize tasks presentation and intraoperative ECoG signal recording, was previously achieved. Hereby, we discuss the testing, validation, and optimization of the system, and present the advanced signal processing and statistical analysis upon which the functional map is formed.

Methods: Data from surgeries (n=3) were collected. The subdural ECoG signals and surface EMG signals were recorded using the Neuro Omega™ (by Alpha Omega). The patient's responses onsets were marked and synchronized with the ECoG signals using a made-from-scratch Arduino-based push-button trigger, and the EMG recordings. MATLAB (by MathWorks) was used for the system control and for signal processing and statistical analysis, alongside with EEGLAB toolbox (by Swartz Center for Computational Neuroscience). Following the signal filtering, epochs around the trigger were extracted. Power spectrograms of the epochs were averaged for each task and electrode, and were normalized to the resting-state preceding the trigger. Thus, presenting the Event-Related Spectral Perturbation (ERSP). For statistical analysis, t-tests were performed to evaluate statistically significant event-related changes in spectral power. The final map was presented based on the counts of significantly changed frequencies in each electrode.

Results: We have succeeded to present a functional map of the patient's cerebral cortex, which emphasizes the task-related differences between the electrodes, and therefore displays the functionalities of different brain regions (fig. 1, b-d). These results were consistent with the ECS results and the literature (fig. 1, e). Also, the ERSP revealed some event-related spectral changes around the response onset (fig. 1, a). This implies that the trigger-aided synchronization is sufficiently precise for our analysis. Moreover, the EMG data proved to be useful in synchronization as well.

Conclusions: The system presented records neural activity (ECoG), synchronizes it to the patient's responses, then creates an intraoperative functional map. So far, we have validated the efficiency of the system in two surgeries. Further data from additional surgeries is needed in order to establish a safe and efficient process using our proposed system.

Keywords: Awake Craniotomy, Electrocorticography, Intraoperative Functional Mapping, Event-related Power Spectral Changes.

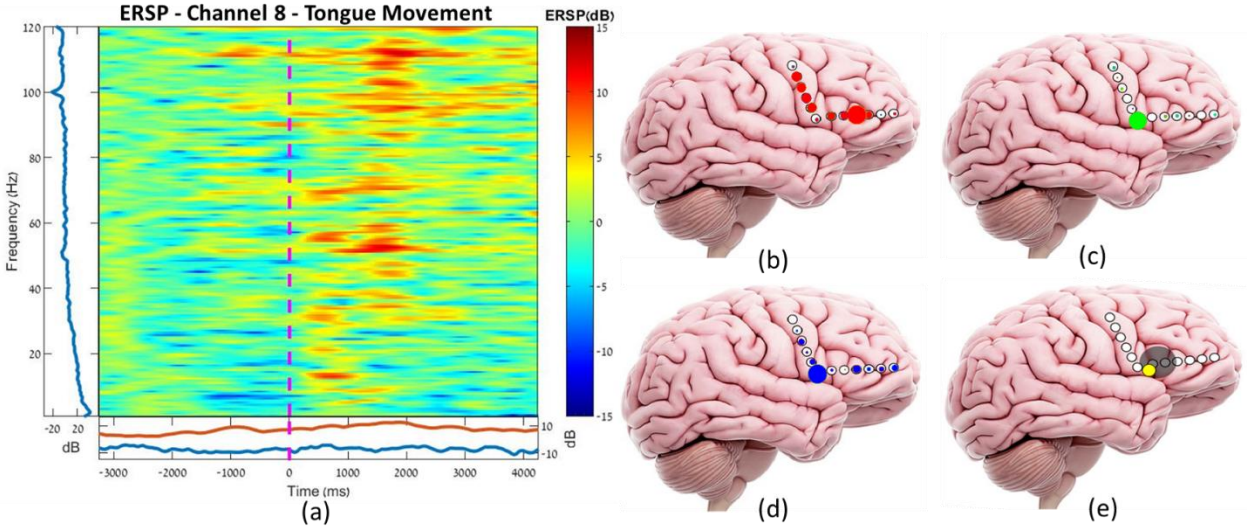

Figure 1: (a) ERSP. Dashed line marks the response onset. (b)-(e) Intra-operative functional map. White circles mark the electrodes locations. Colored circles represent significant task-related activity during: (b) hand movement, (c) Naming task and (d) tongue movement. (e) Gray circle represents craniotomy; yellow circle represents the ECS results.

(10)

An MRI Compatible 3D Printed Split-belt Treadmill for Motor Neuroscience Research

Tania Assaf [1], Wajdi Nicola[1], Ameer Lawen[2], Itamar Kahn[2], Anat Grinfeld[1], Firas Mawase[1]

[1]Faculty of Biomedical Engineering, Technion IIT
[2]Faculty of Medicine, Technion IIT

Introduction: Understanding locomotor adaptation using magnetic resonance imaging allows to identify the structural and functional changes that take place in the neural system. During the last decade, efforts have been made to measure whole-brain activity of awake mice during walking disturbance, the resulting adaptation as well as during motivated locomotion. However, mapping the neural response to behavioral task poses a major challenge including animal handling, MRI restrictive surrounding, fixed scanned head, and filtering blood oxygenation level-dependent (BOLD) noise signals as result of unavoidable animal's head motion under investigation. The lack of tools to study the correlation between the behavioral response and neural activity limited recent studies to suggest a precise functional map of brain's activity during locomotor adaptation.

Methods: To allow measuring whole brain activity during locomotion disturbance and adaptation, we devised an MRI-compatible 3D printed cradle for mice, that incorporates a rotating split-belt treadmill. The treadmill is suitable for the 9.4 tesla animal fMRI, and designed to allow controlling each belt's speed independently, which will induce locomotion disturbance to the mouse. The delicately designed cradle is built from plastic materials while the rotating parts are held in a low friction motion using 15 mm diameter ceramic rotating bearings.

Minimizing animal's head motion during fMRI scanning is done using a headpost which is surgically implanted atop of the mice skulls using dental cement. In our device, we developed a 3D printed bridge that is fixed to our treadmill. The bridge will be used as a headpost holder. Using the stabilizing bridge, we guarantee that the animal will run freely on the treadmill with minimal head motion, thus minimizing head-motion related noise and increasing the reliability of the BOLD signal.

For external control of the treadmill, we purchased two MRI-safe piezo- ceramic motors with their electronics (Nano-motion EDGE4X motors). Although the motors are MR-safe, they cannot be incorporated into the setup inside the scanner's bore, so we placed the two controlling motors outside the small MRI bore and designed a relay system that can transmit the rotating force from the different motors to the treadmill inside the bore.

We used two 75 cm long timing-belts for the coordination between the motors and the corresponding belts in the treadmill.

Results: In our research, we developed a novel platform for probing locomotor adaptation in behaving mice which includes: an MRI-compatible 3D printed split-belt treadmill, MR-safe external continuous rotating control system with predefined and customized motion transmission to the belts. Our system allows creating new locomotor learning surrounding for mice which permits scanning functional neural responses with high temporal and special resolution, minimal head motion and maximal control over the experience.

Conclusions: Our prototype showed that scanning mice in MRI during walking is feasible. The ability to digitally control the speed of the MRI-compatible motors suggests that we can run advanced neuroimaging protocols of motor learning. This open a new niche in motor neuroscience that allows fMRI scanning not only at rest but also during the learning process itself.

Keywords: Locomotor adaptation; split-belt treadmill; MRI-compatible; 3D printing.

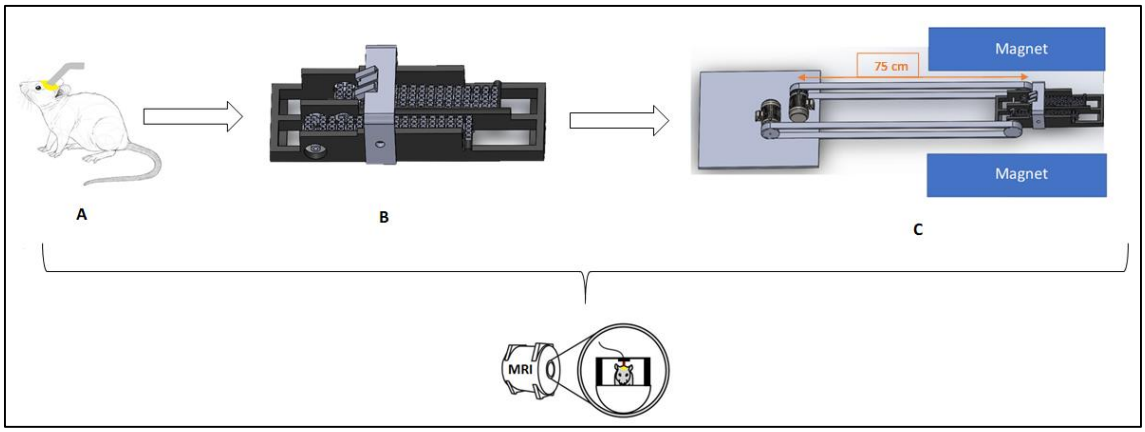

Figure 1: system schematic.
A. Schematic of Investigated mouse with headpost implant.
B. Low friction MRI-compatible split-belt treadmill for mice.
C. Schematic of the displacement of the control system and the motors in the MRI room, using timing-belts for cooperation.

(11)

Reorganization of Functional Networks Following MRI-guided Focused Ultrasound Treatment in Essential Tremor Patients

Daniel Olshvang[1], Or Motzary[1], Firas Mawase[1], Anat Grinfeld[1,2], Gil Zur[2],Noam Bosak[3], Itamar Kahn[4]

[1] Faculty of Biomedical Engineering, Technion IIT
[2] Department of Radiology, Rambam Health Care Campus
[3] Department of Neurology, Rambam Health Care Campus
[4] Faculty of Medicine, Technion IIT

Introduction: Essential tremor (ET) is a progressive neurological disorder that is characterized by a 4 to 12-Hz kinetic tremor in the hands or head and affects approximately 7 million people only in the USA. The tremor probably originates from an abnormality in cerebellar-thalamic loops, suggesting that the disease is a cerebellar outflow disease. Recently, significant clinical success in tremor treatment has been achieved using MRI guided Focus Ultrasound (MRgFUS) ablation of the ventral intermediate nucleus (VIM). Despite success, as a result of the lack of precise characterization of the tremor generating mechanism, the precise mechanism by which MRgFUS ablation succeeds in reducing or eliminating tremor is also not well-understood to date, reducing the ability to properly select the best candidates for this treatment

Methods: A paradigm consisting of 3 periodic separate conditions was created, with a resting phase, a planning phase – where the patient gets ready to squeeze a rubber ball, and an action phase – where the patient preforms the squeeze. A patient with ET that underwent MRgFUS treatment for his right hand 3 months prior, was scanned with an MRI scanner, EMG electrodes connecting to each arm in the Flexor carpi radialis muscle and a tri-axial accelerometer connected to his left hand while following the paradigm. Healthy patient's data was used as control.

The EMG data was cleaned of all residuals using MATLAB and characterizing parameters (AUC, Frequency spectrum and etc.) were extracted and compared with the control values. In addition, Gram-Schmidt orthogonalization was used to separate the variation in tremor intensity from the motor task block vector and to create an rEMG regressor to use for the fMRI data.

The fMRI data collected was pre-processed and underwent statistical analysis using SPM12 to identify activation regions in the brain. The rEMG regressor was used in the

statistical analysis in order to characterize the tremor and identify the tremor triggering regions.

Results: Motor activation on the treated (right) side of the patient showed similar T values in the motor cortex to a healthy subject. EMG parameters were also similar.

Motor activation on the trembling (left) side showed lower T values activations in the motor cortex and showed activations in the Cerebellum. EMG parameters also showed a difference, with a bigger AUC and frequency activation in the range of 5-12 Hz.

In addition, rEMG regressor showed strong activation in Thalamus, although contra-lateral to the side we expected to see the activation in.

Conclusions: EMG signal of ET patients contains information that can help define the variability and severity of the tremor in patients. Furthermore, tremor related activity can be extracted from the EMG, to be further used in fMRI analysis in order to characterize tremor related regions.

Keywords: Essential Tremor; MRI guided Focus Ultrasound, Electromyography

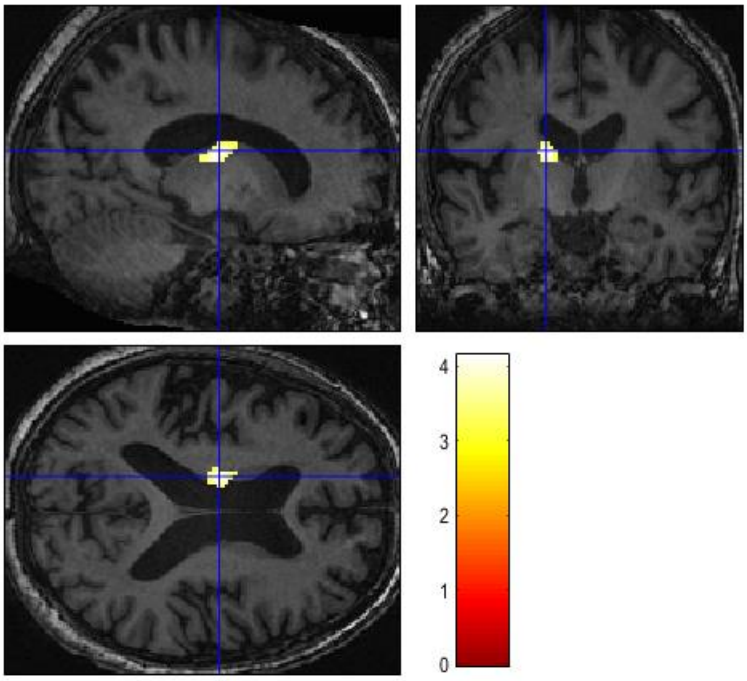

Figure 1: Thalamus Activation due to left hand tremor using the rEMG regressor.

(12)

Identification and Quantification of Synapses from Images of Expanded Brains

Tali Marchevsky[1], Sapir Noah[1], Anat Grinfeld[2], Limor Freifeld[3]

[1] Department of Biomedical Engineering, Technion - IIT, Haifa, Israel
[2] Neuro-Engineering laboratory, Technion IIT

Introduction: Limor Freifeld's lab develop and apply microscopy technology to observe synaptic structure and function based on research of larva zebrafish brains. The main goal is to figure out how nanoscale structures in those brains affect the brain activity and behavior and to use that knowledge to get better understanding of human brains because larva zebrafish brains have neurons and synapses similar to ours.

Using image processing tools that are found on software as MATLAB and FIJI, one can survey the way that the arrangement of proteins in the synapses affects their function. The project is based on images of glycine receptors in glycinergic inhibitory synapses from expanded larva zebrafish brains. The synapses are located on zebrafish's Mauthner cell.

Methods: The original data was composed of four grey scale stacks images. Segmentation was applied on the synapses images by writing unique image processing algorithm and using existing image processing tools available on software.

The image processing course was composed from the following steps:

1. Creating binary image by choosing threshold (TH) manually.
2. Differentiation between objects using connected components (CC) algorithm.
3. Region Growing (RG) algorithm was performed on the original data to reconstruct the missing pixels.
4. Small CC that were found to be too small to represent synapse were removed.
5. K-MEANS Clustering algorithm was performed to separate too large CC (united synapses).

- Each step of the image processing course was followed by manual identification in order to examine the algorithm step and to get the best representation of the original data while keeping high SNR ratio.

Results: Layer 29 of 63 in "pic1" was chosen as a representative layer for manual identification due to its variety of synapses sizes, shapes, and their layout on the cell.

Manual identification results: Small objects (noise) were completely cleared. 47 of 51 (92%) synapses were identified, but only 25 (49%) appeared in the correct way.

Conclusions: Overall, the image processing yielded quite good results. Quantification of synapses shape, size and number of clusters of molecules will be presented later.

To improve the algorithm, there is a need to find more accurate input values for the k-Means Clustering and RG algorithms. Removing CC that are found outside the ROI can be done manually.

Keywords: expansion microscopy, connected components, region growing, k-means clustering.

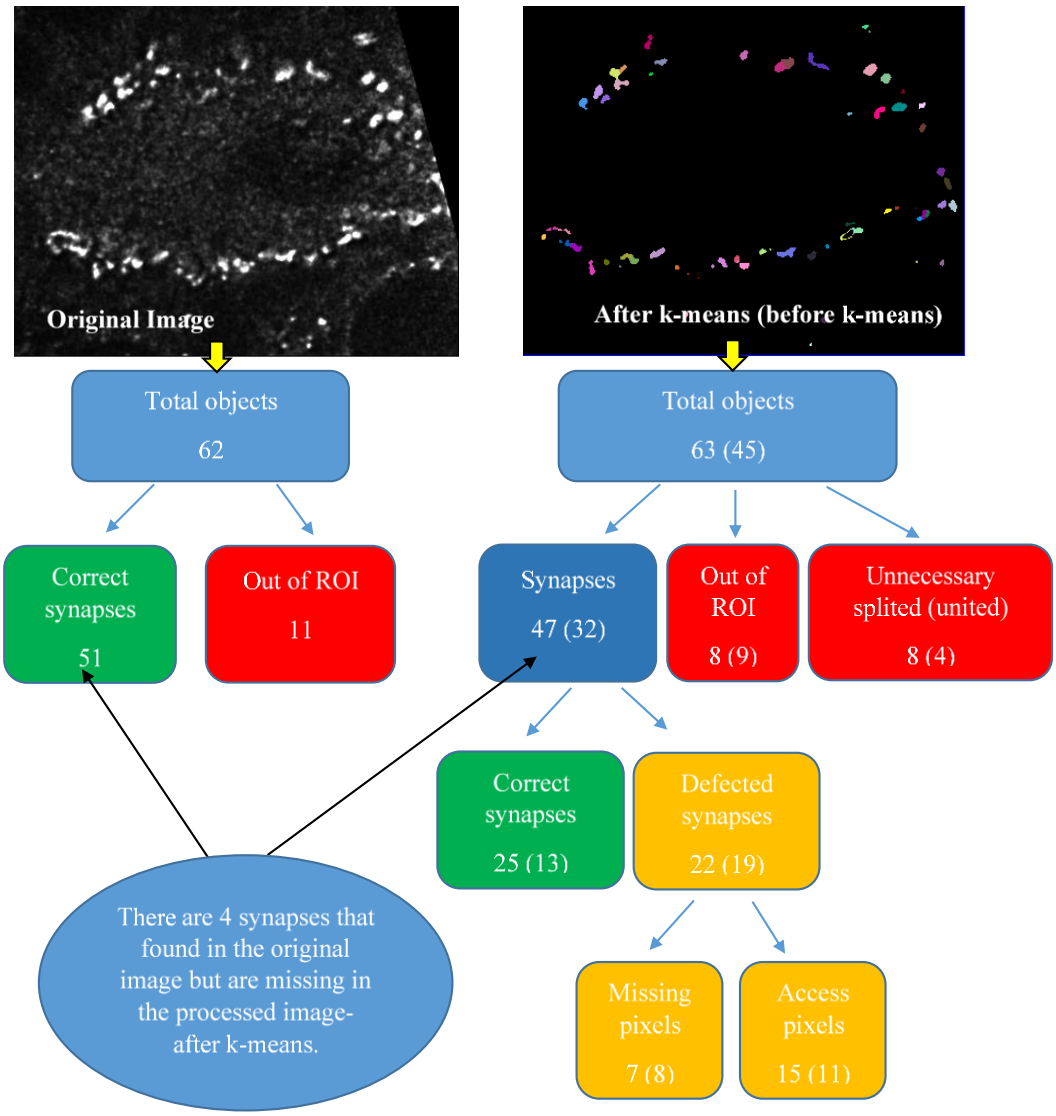

Figure 1: Results of manual quantification vs. automatic segmentation.

(13)

Quantitative DW-MRI analysis algorithms

Judit Ben Ami[1], Marina Khizgilov[1], Anat Grinfeld[2], Moti Freiman[1]

[1] Department of Biomedical Engineering, Technion - IIT, Haifa, Israel
[2] Department of Medical Imaging, Rambam Health Care Campus, Haifa, Israel

Introduction: Intravoxel incoherent motion (IVIM) imaging is a non-invasive MRI technique sensitive to the motion of molecules inside the body. This technique provides several diffusion-weighted MRI (DW-MRI) images, each acquired at different b-value, a parameter that represents the time the particles had to perform diffusion. The attenuation of the signal is assumed to be caused by two biomarkers: slow diffusion, which is associated with cell density, and fast diffusion, which is associated with tissue microcirculation. The total DW signal for each voxel is modeled by:

$$(1)\ s_i = s_0\left(f \cdot e^{-b_i(D^*+D)} + (1-f)e^{-b_iD}\right)$$

Where s_i is the signal obtained with the i^{th} b-value b_i, s_0 is the signal with b=0, f is the perfusion fraction, D^* and D represent the pseudo-diffusion and diffusion coefficients respectively. Together, D, D^* and f are called the **IVIM parameters**. Implementing a post-processing tool that will quantify the IVIM parameters will provide a new, non-invasive, radiation-free diagnostics method in various clinical applications, such as characterization of inflammatory activity in the body (e.g. Crohn's disease), prediction of treatment response, and detection and separation between benign and malignant tumors.

Methods: To quantify the IVIM parameters two approaches were used. First approach is **Least square fitting** – each voxels IVIM parameters are quantified irrespectively to the surrounding voxels. This approach includes three methods: **SEGb** - Segmented Doubly Linearized Least Squares, **SEG** - Segmented Partially Linearized Least Squares, **LSQ** - Full Nonlinear Least Squares. Second approach is **Bayesian Modeling** – each voxels IVIM parameters are quantified respectively to given area of surrounding pixels. The method implemented is **BSP** - Bayesian modeling with a Gaussian shrinkage prior.

Results: A multi-purpose Python library was created which includes: 4 IVIM parameters estimation algorithms, phantom creating function, and error calculation functions. In addition, for efficiency and higher performance, the library uses vectorize programming, multiprocessing, assertions and exceptions. DW-MRI images from Boston children's hospital databases were analyzed and IVIM parameters maps were estimated. Reconstructed (with eq. 1) images gave an average (STD) error of 17%.

Link to Projects page on TCML website: https://tcml-bme.github.io/Cproject.html#proposal3

Conclusions: Quantification of fast and slow diffusion from DW-MRI data is challenging due to the low SNR and the large number of variables compared to the number of observations, but is possible using the approaches mentioned above. Bayesian modeling is capable of producing more visually pleasing IVIM parameter maps than least squares approaches, but their potential to mask certain tissue features demands caution during implementation.

Keywords: Diffusion-Weighted MRI, IVIM Parameters, Model fitting algorithms, Python library.

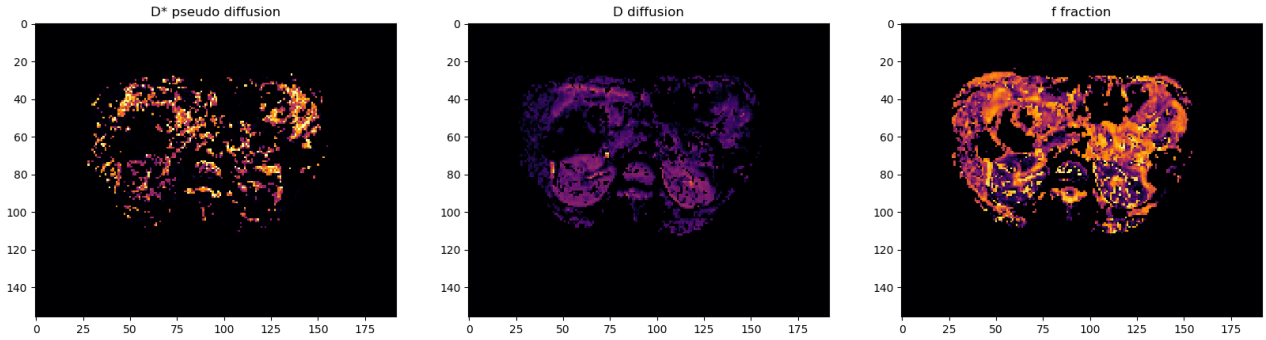

Figure 1: Estimated IVIM parameters maps using LSQ method. Diffusion-weighted MRI of kidneys was performed. By applying intravoxel incoherent motion (IVIM)–based biexponential analysis IVIM maps were estimated: diffusion coefficient (D), which reflects tissue diffusivity; pseudo-diffusion coefficient (D*), which reflects microcapillary perfusion; and perfusion fraction (f).

(14)

Visualization Software for Pediatric Crohn's Disease Assessment by Multi Planar Reformation

Yael Zaffrani[1], Anat Ilivitzki[2], Anat Grinfeld[1], and Moti Freiman[1]

[1] Department of Biomedical Engineering, Technion - IIT, Haifa, Israel
[2] Radiology Unit, Ruth Rappaport Children's Hospital, Haifa, Israel

Introduction: Crohn's disease (CD) is a chronic inflammatory transmural disease of the bowel. The inflammation is discontinuous leading to segments of inflammatory exacerbation and regression throughout the gastrointestinal tract. CD can affect any part of the gut, but the terminal ileum is the most frequent localization. One approach for diagnosis of CD is MRI enterography (MRE). MRE allows for a detailed evaluation of the bowel and has emerged as an effective method for imaging the, hard to reach, small bowel in patients with CD. MRE is especially useful for pediatric CD patients as doctors strive to spare children the potentially harmful effects of radiation. However, visualization and quantification of disease burden requires constant scrolling, back and forth, through 2D images to follow the twisting anatomy of the bowel, making it difficult to fully appreciate the extent of disease. In this work, we demonstrate a new open source based software tool that enables the visualization of the curved gastrointestinal tract on a single image, using a multi planar reformatting (MPR) algorithm.

Methods: We implemented a Software in Python®. The software enables the visualization of conventional anatomic plans: sagittal, coronal, and axial using the VTK library. The radiologist is able to fully interact with the images by mouse and keyboard such as: zoom in/out, slicing through 2D conventional images, and contrast control. To generate the MPR view, the radiologist needs to first place seed points in the most visible cross-section along the curved lumen. Using the seed points, an algorithm extracts a center line along the curved lumen. To preform center line extraction, we compare three algorithms: linear interpolation, spline interpolation, and shortest paths algorithms. We construct the MPR view from the extracted center line, using the algorithm described by Kanitsar et al. The software allows disease extent measurements on both, standard and MPR view, approaches.

Results: We have created a practical and stable visualization software implemented in Python®. The software provides a comprehensive and clear depiction of the disease state on a single image by extracting the MPR view. Our hypothesis is that MPR view allows for a more accurate measurement of involvement length, which is a quantitative biomarker useful for assessing CD. To test this claim, we will conduct a clinical trial comparing standard and MPR measurements from pediatric subjects with verified CD.

Conclusions: Quantitative measurements of CD are required when assessing medical therapeutic responses or making decisions for surgical treatments. MPR views provide a better depiction of the disease state on a single image. By assessing the disease using MPR view, the radiologist will be able to perform more accurate measurements without scrolling back and forward through 2D images.

Keywords: Crohn's disease, MRE, MPR

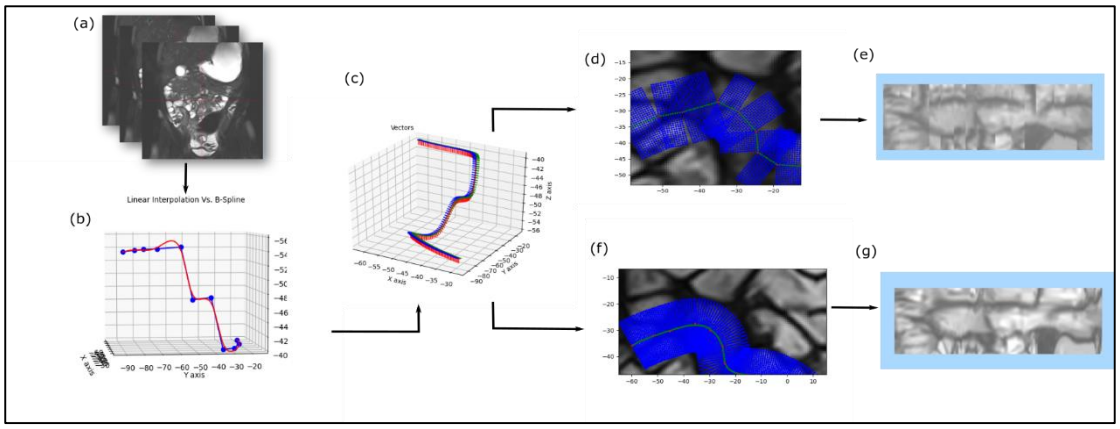

Figure 2: Demonstration of the software workflow: (a) seed points in 2D conventional images. (b) lumen center-line extraction. (c) MPR planes extraction. (d) linear interpolation. (e) MPR linear visualization of the lumen. (f) spline interpolation. (g) MPR spline visualization of the lumen.

(15)

Develop of Diagnostic System for Preventing Sudden Cardiac Death among Athletes

Matti Zeev[1,2], Nimrod Baram[1], Ido Weiser Bitoun[1,2], Alexandra Alexandrovic[1], Michal Zivan[1], Yeal Yaniv[1]

[1] Faculty of Biomedical Engineering, Technion - IIT, Haifa, Israel
[2] Faculty of Medicine, Technion - IIT, Haifa, Israel

Introduction- Sudden Cardiac Death (SCD) is a pathological phenomenon characterizes by fatal loss of heart function. In many cases it is caused by cardiac failure derived from genetic disorder. Some of these genetic disorders are expressed with Bradycardia, which is a low resting heart rate (less than 55 beats per minute). Among athletes, there is another phenomenon, non-pathological, called Athletic Heart Syndrome (AHS), which is a low resting heart rate due to cardiac physiological changes. Although athletes undergo physical and electrocardiography (ECG) tests routinely, in case of genetic disorders that cause bradycardia among athletes, it may be misdiagnosed as AHS. Genetic tests are inaccessible, expensive and do not performed during athletes' routine functional health tests. However, by using cardiac signal analysis, we can identify the cardiac function. Such method is analysis of the heart rate variability (HRV)- a term represents the momentary variation of the heart rate between two consecutive heart beats- may indicate on heart failure. HRV changes in cardiac pathologies and can enable us to diagnose such pathologies and even cardiac genetic disorders.

Methods- we compared between 6 athletes and 9 non-athletes ECG data before, during and after physical exercise. Additionally, we analyzed ECG data of patients having genetic disorders affecting the heart: 4 carriers of mutation in the hyperpolarization-activated cyclic nucleotide-gated channel 4 (HCN4) gene and 5 carriers of mutation in sodium voltage-gated channel alpha subunit 5 (SCN5A) gene, the both mutations cause to bradycardia. We compared these data to 20 patients from another data, with normal sinus rhythm (NSR) in rest mode, and to the athletes and non-athletes that mentioned before in rest mode only, all defined as healthy group.

We used our knowledge derived from the ECG analysis and developed a diagnostic system for cardiac mutations among athletes, which includes ECG recorder and a real time novel algorithm implemented in LabView graphical user interface. Given an ECG signal, our system finds the R peaks using PhysioZoo tool box and based on its intervals analyze the variability of the heart rate using statistic features. Based on these features, we defined 2 classifiers- to distinguish between healthy and non-healthy, and within the non-healthy to distinguish between both mutations. Finally, we tested every member of the data sets according to the classifiers.

Results- comparing the characteristics difference between athletes and non-athletes in rest, exercise and recovery modes, we found that the heart pacemaker among athletes functions differently from non-athletes during rest and physical activity, and therefore there are differences in HRV between them both. Based on our findings, we can measure the 'degree' of patient athleticism. Moreover, we analyzed the Multiscale entropy (MSE) of healthy subjects and patients having the mentioned genetic mutations. MSE calculated on the signal by dividing it to sections, each section contains n samples- when n represents the scale. The MSE plot is the entropy as a function of the scale. We found that there is difference in the low and high scales of the MSE between the groups.

By analyzing our ECG data, we were able to distinguish between the each of the four groups by the mentioned classifiers, with high accuracy and precision, as displayed on table 1.

Group	Number of participants	TP	TN	FP	FN	Accuracy	Precision
Health Non-athletes	29	29	0	0	0	100%	100%
Athletes	6	5	0	0	1	83%	100%
Sick1-SCN5A	5	0	5	0	0	100%	100%
Sick2-HCN4	4	0	4	0	0	100%	100%
Total	44	34	9	0	1	97.60%	100%

Table 1: prognosis distribution.

Conclusions- the algorithm we developed can identify healthy athletes and non-athletes as well as patients with two cardiac pathologies (HCN4, SCN5A) based on 10 min of ECG recording. With more cardiac pathologies analysis, our diagnostic system can be used as part of athlete routine functional health tests and may reduce the cardiac morbidity and mortality among athletes.

Keywords- Heart Rate Variability, Bradycardia, Athletes, Sudden Cardiac Death.

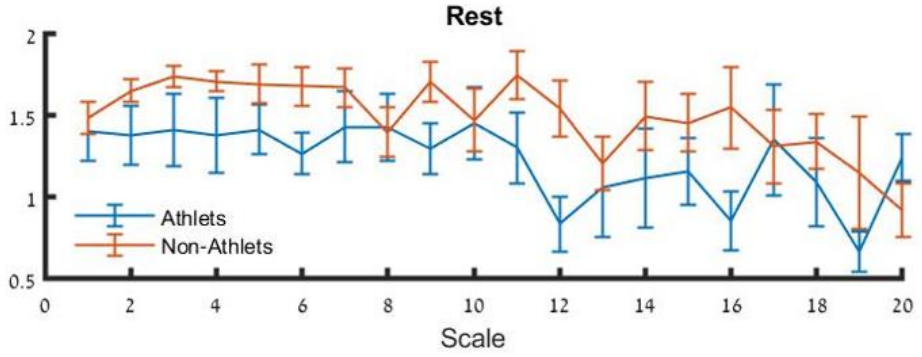

Figure 1: Multiscale entropy (MSE) plot emphasizes differences between athletes and non-athletes HRV (on rest mode).

(16)

Detecting heart abnormalities using a novel platform of digitized 12-lead ECG

Nitzan Avidan[1], May Buzaglo[1], Vadim Gliner[2], Yael Yaniv[1]

[1] Biomedical Engineering Faculty, Technion - IIT, Haifa, Israel
[2] Computer Science Faculty, Technion - IIT, Haifa, Israel

Introduction: Standard 12-lead Electrocardiogram (ECG) is a graphical representation of the electrical activity of the heart and is used as the primary clinical tool to detect abnormalities in heart function. Currently, the ECG is printed as an analog signal on a thermal paper and is analyzed by cardiologists only. A reliable automatic diagnostic tool for 12-lead ECG recordings is required to provide a second opinion for health care providers and also to provide a simple, fast and accessible tool for the general population to detect cardiovascular conditions.

Methods: Captured 12-lead ECG paper plots, using smartphone camera, were used as an input for a mobile application for classification of 12-lead ECG data paper. These images can either be converted to a digital signal in the form of vectors or remain in their original form. Each method serves as a direct input for advanced machine learning and artificial intelligence (AI) algorithms. The first method of extracting ECG signal vectors is a challenging task, as it must deal with artifacts caused by mobile device image acquisition. This method might damage the signal and consequently lead to results with low accuracy. The second method requires a very large dataset of ECG images, however the signal does not damaged. For applying the second method we generated ECG images database. Our database includes 79k ECG images approved by cardiologists, 40% of them are classified as normal sinus and the rest are classified as one or more of cardiovascular disorder types. In addition, a general information including meaningful relevant ECG features (e.g. heart rate, axis etc.) of each image was saved for future use and calculations. For a start, we tested the performance of the application on atrial fibrillation (AF), one of the most common cardiovascular conditions. In addition, to examine how the system deals with camera artifacts (e.g. shadow, rotation etc.), we scanned tens of ECG papers with two different smartphone cameras.

Results: For AF detection, we received 100% accuracy for a set of 10 images: 5 of normal sinus and 5 of AF. Similar degrees of accuracy were achieved with images as compared to digital vectors input signals (96%). In addition, identification of ECG images with artifacts and distortions were a bit less accurate than without (Figure 1).

Conclusions: In the age of smartphones and Internet of Things, accurate automatic device that can be found at any clinic and even can be within reach is an essential tool for detection of cardiovascular diseases. Our database was essential part of this research and contributed to the creation of a highly accurate classification platform of different cardiovascular diseases types. Application results indicate the way forward for future work, which could allow a novel tool for diagnosis of ECG papers.

Keywords: Atrial Fibrillation; 12-lead ECG; Cardiovascular Disease; Machine Learning; Internet of Things, Artificial Intelligence, Heart abnormalities, Heart failure.

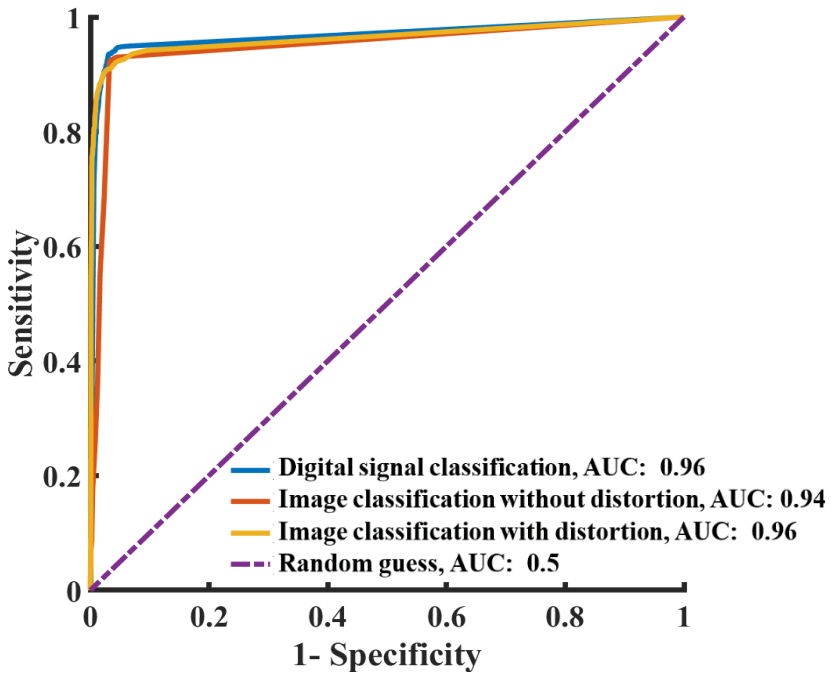

Figure 1: The receiver operation characteristic (ROC) of atrial fibrillation detection.

(17)

Development of a Non-Invasive Clinical Tool for Analyzing SAN & ANS Function and Identifying Cardiac Pathologies

Opal Nimni, Ayelet Lotan, Ido Weiser-Bitoun, Yael Yaniv

Faculty of Biomedical Engineering, Technion – IIT, Haifa, Israel

Introduction: The sinoatrial node (SAN) is the primary pacemaker of the heart, and together with the effect of the autonomic nervous system (ANS), they control the heart rate. Analysis of the heart's biological signals enables us characterization of the SAN activity and identification of diseases and pathological conditions, such as sinus node dysfunction and cardiac arrhythmias. The current methods used to diagnose SAN pathologies are invasive or require a physician to decode the test results. Therefore, we developed a portable and non-invasive clinical tool for assessing the SAN and ANS function and diagnosing cardiac pathologies.

Methods: We obtained electrocardiogram (ECG) data from dogs, rabbits, rats and mice, in basal and denervated state as a pre-clinical analysis, and human ECG data of healthy individuals and chronic heart failure (CHF) patients.
We performed the ECG analysis using the PhysioZoo platform and calculated 27 different heart rate variability (HRV) measures, estimated from the RR (R wave to R wave) intervals. The calculation is based on the time domain, frequency domain and nonlinear methods. Additionally, the analysis includes the multiscale entropy rate (MSE), which is based on Sample Entropy and enables us to identify the SAN and ANS activity. Using the MSE values, we compared between the different mammals and humans both in healthy and pathological conditions. Subsequently, we created a normal human range of the MSE values, which we used to develop our algorithm to diagnose SAN and cardiac pathologies. We implemented the algorithm in an Android application wirelessly connected to a portable pulse watch that serves as a diagnosis and monitoring tool for patients.

Results: Following the comparison between the different mammals, we concluded that there is a significant difference between the human and small mammal cardiac physiological signals. In contrast, we discerned a similarity between the human and dog features. Therefore, the understanding of the dog SAN and ANS signature as seen in the signal, contributed to our knowledge of the cardiac electrophysiological mechanisms, hence applying it during the development of the diagnostic algorithm. We concluded that the ANS affects the low scales of the MSE values, as the SAN affects the high scales.

The human data were divided into five groups by sex and age to avoid influence of these parameters on the analysis. For each group we created a normal range for the MSE values, based on the comparison between human normal and CHF MSE at the relevant scales. We used the defined ranges to create our diagnostic algorithm, and we implemented it in the mobile app that communicates with a pulse watch.

Conclusions: The clinical tool we developed calculates the patient's MSE, basing on RR intervals and tests whether the values are found within the normal human range. Our mobile app reports the heart rate, SAN and ANS function, and whether there is a suspicion of CHF. This tool enables the identification of pathological conditions in an accessible and non-invasive manner.

Keywords: heart rate variability (HRV), electrocardiogram (ECG), Cardiac Pathology Diagnosis, Mobile Monitoring.

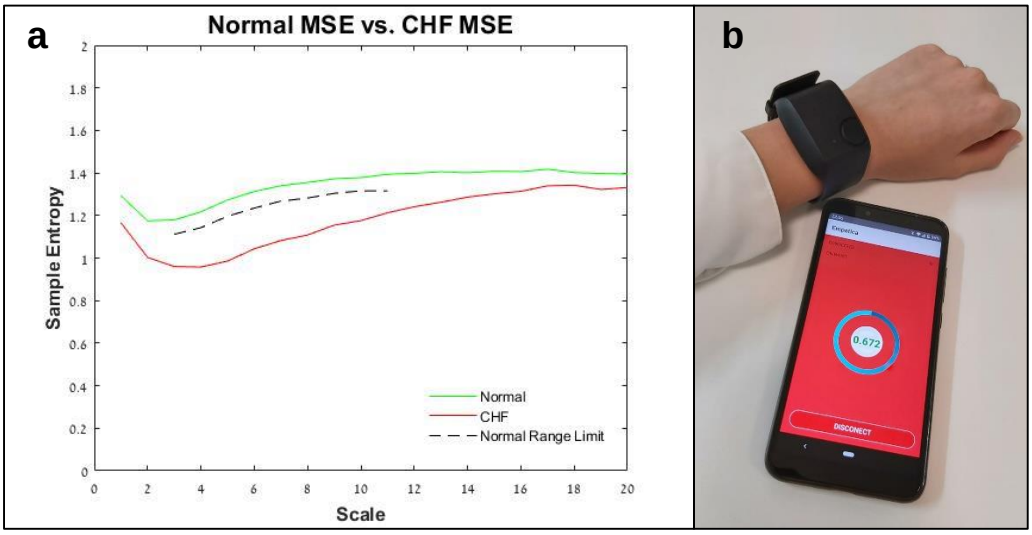

Figure 1: (a) Normal MSE vs. CHF MSE for the group of 60-80 years old women shows our algorithm cutoff values enables us the diagnosis, (b) The android application and pulse watch used as our non-invasive clinical tool.

(18)

MRI Brain Tumor Segmentation

Shany Biton, Zohar Avinoam, Anat Grinfeld, Moti Freiman

Biomedical Engineering Faculty, Technion - IIT, Haifa, Israel

Introduction: Glioma is a type of tumors that starts in the glial cells of the brain or the spine. Gliomas are the most frequent primary brain tumors in adults and despite considerable advances in glioma research, patient's diagnosis remains poor. The clinical population with the more aggressive form of the disease, have a median survival rate of two years or less and require immediate treatment. To evaluate the progression of the disease and successfully choose treatment strategy, intensive neuroimaging protocols must be used. Nowadays, the most common method to evaluate is a basic quantitative measurements and contrast enhancement characters. Current methods are time consuming, manually handled, and subjective.

Methods: We designed two models: both models are based on an U-net architecture inspired by encoder-decoder structure of Convolutional Networks (CNN) with strategy that relies on the strong use of data augmentation to use the available annotated samples more efficiently. In the first model we added the variational autoencoder (VAE) branch to the network to reconstruct the input images jointly with segmentation to regularize the shared encoder.

In the second model we introduced the Mixed Structure Regularization (MSR) by implicitly encourage the model to learn a sparse representation by stochastically corrupting the input data with randomly added structure sampled from the training dataset and additive Gaussian noise.

For the Brain tumor segmentation, the models were trained on BraTS 2018 dataset of glioma patients (219 cases) and then validated on separate dataset (66 cases).

We concatenated 4 available 3D MRI modalities into the 4-channel image as an input. We normalize all input images to have zero mean and unit std and applied Data augmentation to teach the networks the desired invariance and robustness properties. We used a hierarchical training approach, in which the number of minibatches, the number of epochs, and the learning parameters were modified at each stage to accelerate and stabilize the convergence of the training procedure. A minibatch size of 32 samples was used for all stages. We optimized the value of the hyperparameters of each network. The output of the network is 3 nested tumor subregions.

Results: For brain tumor segmentation, the U-net and MSR models' scores are summarized in Table 1:

Model	L-Dice	Hard Dice	IOU
U-net	0.119 ± 0.009	0.864 ± 0.009	0.769 ± 0.013
MSR, σ= 0.1 %	0.045 ± 0.004	0.917 ± 0.005	0.854 ± 0.007
MSR, σ = 1%	0.137 ± 0.017	0.844 ± 0.018	0.748 ± 0.024
MSR, σ = 0.5%	0.184 ± 0.016	0.798 ± 0.013	0.688 ± 0.014

Conclusions: Adding the regularization methods have changed the learning curve and influenced the segmentation determined by it.
For brain tumor segmentation, the MSR model performed best with σ= 0.1 %. AE model performed poorly, thus we decided to exclude its result.
These results indicate a possible progress in brain tumor diagnosis and treatment that could benefit both the patients and the doctors.

Keywords: MRI, Brain, Image segmentation, Deep sparse overcomplete autoencoder, Regularization.

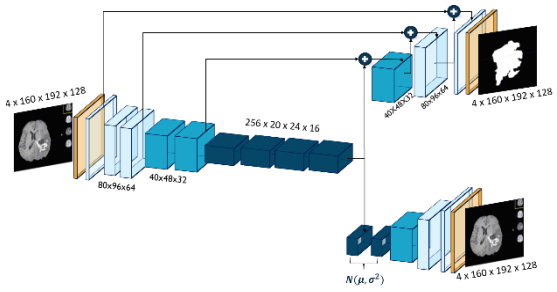

Figure1: MSR model architecture.

(19)

Brain Tumor MRI Image Segmentation

Michaela Ayoun, Moti Freiman, Anat Grinfeld

Biomedical Engineering Faculty, Technion - IIT, Haifa, Israel

Introduction: Gliomas are the most common primary brain tumors in adults, presumably originating from glial cells which surround neurons in the brain, gliomas grow within the substance of the brain and blend with healthy tissues. Despite advances in glioma research, patient diagnosis remains poor. The part of the population who is most susceptible to the more aggressive form of the disease, high-grade gliomas, have an expectancy of two years or less and require immediate treatment. Whereas, low-grade patients, have a life expectancy of several years. Therefore, aggressive treatments are often postponed as far as possible. For both grades, neuroimaging methods are used during treatment to evaluate the progression of the disease and the success of a specific treatment strategy. Today, neuroimaging is evaluated with professional observation of the scanned image, this method is time consuming, inefficient, and subjective. These basic current assessments can be replaced with highly accurate measurements of the tumor substructures.

Methods: We implemented a Deep Learning Convolutional Neural Network Algorithm for MRI tumor segmentation. We used the MICCAI BRATS 4D multi-channel dataset, the segmentation was done on four annotations of different clinical use – Edema, Non-Enhancing, Necrotic core, Non-Enhancing core. As well as three regions– whole tumor, tumor core, active tumor.

First the segmentation was done by implementing the U-net algorithm, A network and training strategy which relies on the use of data augmentation, as in the clinical world, to use the available annotated samples more efficiently. The U-net results were after refered as the ground truth for the Sparse Autoencoder innovation added.

Autoencoders try to learn an approximation to the identity function of correlated features of the data. representations learnt in a way that encourages sparsity, obtain improved performance on classification tasks. The implementation was done by imposing constraints on the hidden units of the U-net. Sparsity constraint forces the model to respond to the unique statistical features of the input data. The sparse autoencoder involves a sparsity criterion penalty, that encourages the model neurons to activate specific areas of the network, while forcing all other neurons to be inactive. This sparsity of activation was achieved by formulating the penalty terms done with the Kullback-Leibler (KL) divergence. After the training with the sparse algorithm the results were analyzed with three accuracy criterions.

Results:

Sparse AE	L dice	Hard dice	IoU
train	0.031	0.93	0.872
test	0.126	0.848	0.745

Evaluation metrics: Sørensen - Dice coefficient, Hard dice and Jaccard coefficient – Intersection Over Union (IoU).

Conclusion: The Sparse Autoencoder can Improve the ability of generating a more accurate segmented image. The first results were very close to the U-net outcome, the existing method today, and even more accurate. With more optimization the accuracy can even improve. Resulting with better diagnosis and early detection, and increased effectiveness and efficiency of a treatment.

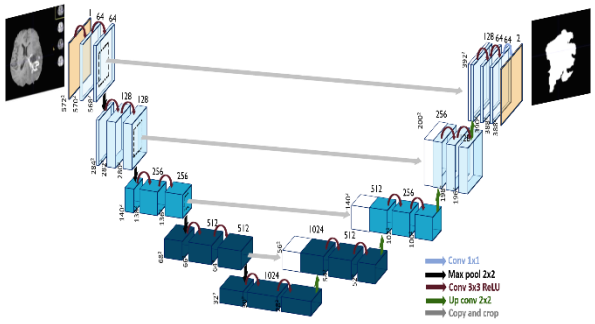

Figure1: U-net algorithm

(20)

Feasibility of Ultrasonic Thermal Monitoring Using Coded Excitations for Focused Ultrasound Hyperthermia

Noy Parti, Tomer Romano, Daniel Dahis, Haim Azhari

Department of Biomedical Engineering, Technion - IIT, Haifa, Israel

Introduction**:** Focused Ultrasound (FUS) is used for thermal treatments. It offers a non-invasive and effective procedure to treat neurological diseases such as brain tumor and essential tremor. The current treatments include Magnetic Resonance Imaging (MRI) temperature monitoring during FUS ablation. Although MRI shows high efficiency and accuracy It has several limitations such as limited accessibility and high cost. Acoustic thermal monitoring could provide alternative approach that will lower the cost and increase the accessibility. However, brain ultrasonic monitoring is challenging due to the skull bone attenuation and induced aberrations, which substantially reduce the waves signal-to-noise ratio (SNR). Coded Excitations (CoE) is a methodology which could potentially overcome these challenges. Hence the main aim of this study is to evaluate the feasibility of using Golay CoE sequences for non-invasive temperature monitoring of brain tissue while using the therapeutic FUS transducer itself.

Methods: A variety of Pre-prepared complementary Golay sequences were tested using High Intensity Focused Ultrasound (HIFU) transmission method. The most suitable Golay sequence was chosen using MATLAB simulation, and it was used to provide an amplified narrowed signal, even under poor SNR conditions. A FUS transducer manufactured by INSIGHTEC was used to transmit 1 MHz signals. The FUS was positioned in a water tank. A 3D holder was printed and mounted on top of the transducer. After preliminary experiments, Plastic containers were filled with ex-vivo bovine brain tissue (white matter and cortical matter) resected from the cortex. Next, the containers were heated to about 45^{o}C, by immersion in a water-filled beaker. Each container was then positioned in the focal zone of the system and sonicated with Golay sequences every 1 second during cool down, until reaching 30^{o}C. Three thermocouples were used for real-time temperature monitoring of the samples. From the obtained decoded signals, the echo shifts trajectories as a function of temperature were registered.

Results**:** After the analysis of the echoes by Coded Excitation, we were able to see improved SNR of the Golay-derived signal in comparison to the raw RF echoes. Furthermore, high linear correlation between the estimated normalized white matter Speed of Sound (SoS) and temperature was observed- while in the cortical matter high correlation was observed between the SoS and temperature to a 3-degree polynomial fit. Furthermore, in the follow experiment a bone was inserted

in order to mimic the skull and a correlation was found between the white matter SoS (See figure 1) and temperature. This indicates the validity of the assumption and the possibility of obtaining noninvasive brain tissue temperature estimation using CoE.

Conclusions**:** The feasibility of CoE-mediated acoustic thermal monitoring using a single FUS transducer for transmission and reception was successfully demonstrated. Importantly, the echo-shift trajectories as a function of temperature indicate the possibility of temperature estimation.

This approach can serve as a basis for the development of a new tool for brain FUS thermal monitoring, without the use of MRI.

Keywords: Focused Ultrasound, Coded Excitation, Thermal Monitoring.

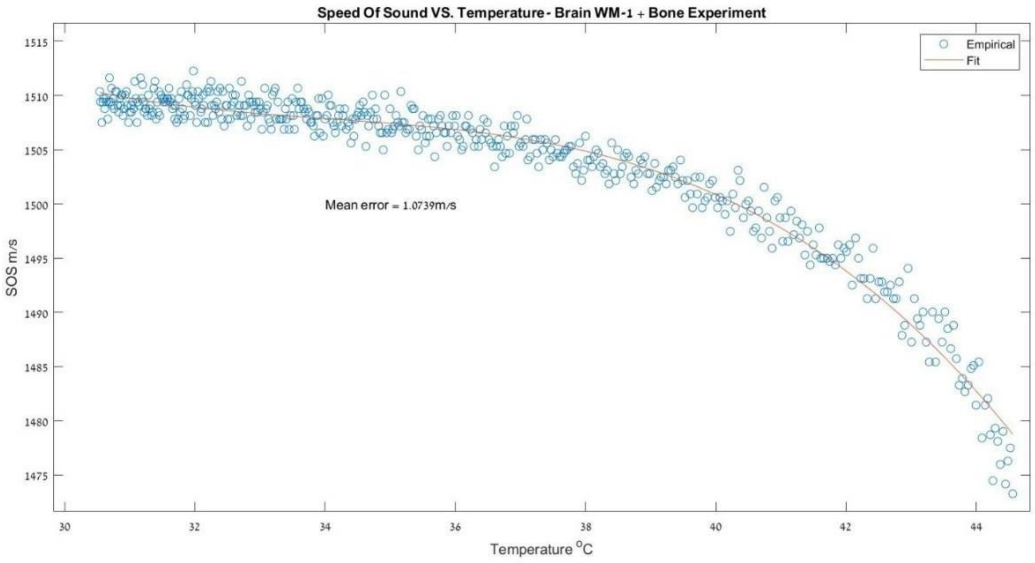

Figure 1: SoS VS Temperature in brain white matter +Bone.

(21)

Disease diagnosis based on Bio markers
Using tagged proteins transport through Nano-Pore system and Machine learning

Maya Eytani, Oren Shorr, Michal Zivan, Shilo Ohayon, Amit Meller

Faculty of Biomedical Engineering, Technion IIT

Introduction: Early disease diagnosis is of great importance and can highly impact a patient's life quality and reduce the required medical procedures. Many diseases are only diagnosed at a relatively late stage, when major symptoms appear, and the possible treatments become limited. Recent studies suggest that some disease can be diagnosed at a very early stage through detection of certain biological changes that occur in the body in the early phase of the disease, some of these changes include the presence of disease specific biomarkers, those are either new molecules that are produced in the body, or existing molecules that change their relative concentration upon disease onset. Early diagnosis can be achieved by detecting these biomarkers.

The system we based our project on is a nano-pore sensing system. The core idea of this method is to tag specific amino-acids within the protein each by a different emission spectra fluorescent dye, then using SDS and electric bias let these proteins translocate one by one through a nano-pore, excite the nano-pore exit and collect the emitted signal (see Figure 1). These signals withhold information regarding the number of each tagged a.a as well as their order of appearance in the protein – that information is used to classify the protein translocated.

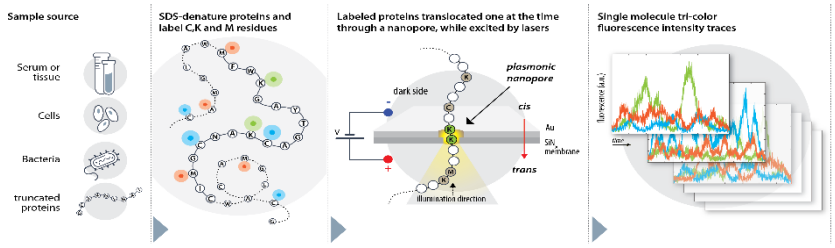

Methods: Focusing on two main diseases - Alzheimer and SARAS2-covid19, we gathered information about possible protein biomarkers for these diseases and the protein concentrations in a patient's typical sample. Using a dedicated pre-developed MATLAB APP of the nano-pore system, we generated a dataset of saliva samples containing SARAS2-covid19 proteins with varying concentrations, in optimal laboratory conditions and average laboratory conditions, as well as Plasma samples of healthy patients, Symptomatic and Asymptomatic for Alzheimer patients. The samples have been fed to a trained Support Vector Machine (SVM) saliva protein classifier

and SVM plasma protein classifier respectively, the latter one's output was then fed to a trained Random Tree classifier, which decided if a sample is from a healthy, symptomatic or asymptomatic patient. Furthermore, we developed an algorithm to use as a pre-processing step to normalize the optical trace signals before feeding them to the classifiers.

Results:

SARS2-Covid19 protein classification: In optimal laboratory conditions and tagging a.a combination of C, K & M, one protein had consistent F-measure>80% and another with F-measure > 70%. At Average conditions only one protein kept on consistent F-measure>90%, and the high recall of the 2 previous proteins was unfazed.

When tagging a.a C, K & V, 4 out of 13 SARS2 proteins had consistent high recall (>89.8%) ,2 proteins with consistent F measure>90%, one with F-measure>85% and another with F-measure>80%. At Average conditions 2 proteins had consistent F-measure >80% and >90%.

Generally, the performance of classifying SARS2 13 proteins of the model improved comparing to CKM tags.

Whole plasma sample Alzheimer Random Tree classifier: The precision recall and F-measure of the Random Tree all greater than 90% when focusing on the different combination of the groups healthy, symptomatic and asymptomatic.

Data pre-processing: The goal of this stage was to normalize optical trace signals that were produced by different instances of the same protein type that translocated through the nano-pore at different velocities, and therefore have different number of samples. Mean Squared Error (MSE) of the original signals & normalized signals were calculated (from the ground truth signal) in optimal conditions and there was an ~80% decrease in MSE for the normalized signals. Furthermore, the new normalized signals retained most of the original and critical information.

Conclusions:At the signal protein molecule identification, it is possible to improve recall, sensitivity and F measure by tagging different amino acids combination. While tagging CKV, there are 2 strong biomarkers for SARS2-Covid19 with high parameters in optimal and average conditions and could be used in future diagnostic applications.When looking at the whole sample proteome and known biomarkers, Nano-pore systems combined with machine learning methods have potential assisting in early diagnosis of diseases such as Alzheimer.

Keywords:Nano-Pore, Alzheimer, SARS2, Covid19, Signal normalization, Machine learning, SVM, Random Tree.

(22)

Laser Speckle Contrast Imaging in Biomedical Optics

Arseny Belousov[1], Dmitry Rudman[1], Yokhay Dan[2], Michal Zivan[1], Rami Shinnawi[2]

[1] Biomedical Engineering Faculty, Technion - IIT, Haifa, Israel
[2] AntiShock (MindUP), Haifa, Israel

Introduction: Annually, in US, 4.3M critically ill patients in intensive care unit with various diseases are adversely affected by non-personalized intravenous fluid administration procedures. Fluid overload increases mortality, morbidity, re-admission, and medical intervention usage rates. The current medical practices fail to detect the exact amount of fluids each patient needs. Macrohemodynamics parameters in large blood vessels (such as blood pressure and cardiac output), doesn't necessarily reflect the blood flow down the road in the small blood vessels, which lead blood into vital organs.

Methods: Most of the techniques which have been developed for imaging of tissue perfusion exploit the interference pattern generated from diffusely backscattered light from the skin, also called - speckle pattern. When there is movement in the object, the speckle pattern will change over time. This changing speckle pattern is recorded with a camera that has a long integration time compared to the typical decorrelation time of the speckle pattern, as a result, the speckle pattern will be blurred in the recorded image. The level of blurring is quantified by the speckle contrast. If there is no or little movement in the object, there will be no or only a little blurring. Quantitative interpretation of the data from such measurement schemes often hinges on accurate knowledge of the spatial and temporal statistical behavior of the speckle phenomenon. To complement experimental measurements, we turned first to computer simulation of the phenomenon, which allowed us to determine algorithmically the parameters of interest: speckle size, spatial and temporal contrast, decorrelation and integration times.

In order to measure particle speed experimentally, we build a setup for simulation of capillary blood flow using a syringe pump and a microfluidic chip. Our imaging system comprised of focusing optics, a variable diaphragm and a CCD sensor. The area of interest was illuminated with a coherent laser ($\lambda \cong 650$.) The digital photography was processed by the computer and the local contrast was computed in spatial and temporal manner.

Results: Number of laser speckle contrast techniques were implemented and analyzed with our setup and algorithms.

Technique	Abbrev.	Domain	Principle
Laser speckle contrast analysis	LASCA	Spatial	Contrast is determined in 1 image over 5x5 or 7x7 pixels.
Laser speckle imaging	LSI	Temporal	Contrast is determined in 1 pixel over 25 or 49 images.
Laser speckle perfusion imaging	LSPI	Spatial & Temporal	Combination of LASCA and LSI.
Gaussian kernel laser speckle contrast analysis	gLASCA	Spatial	Processes the raw images primarily with the Gaussian kernel operator along the spatial direction of blood flow.

Each technique has its benefits, the selection depends on purpose. In Figure 1 we show results from LASCA algorithm obtained with our setup. Under the assumption of a velocity distribution speckle contrast related to particle speed and decorrelation time.

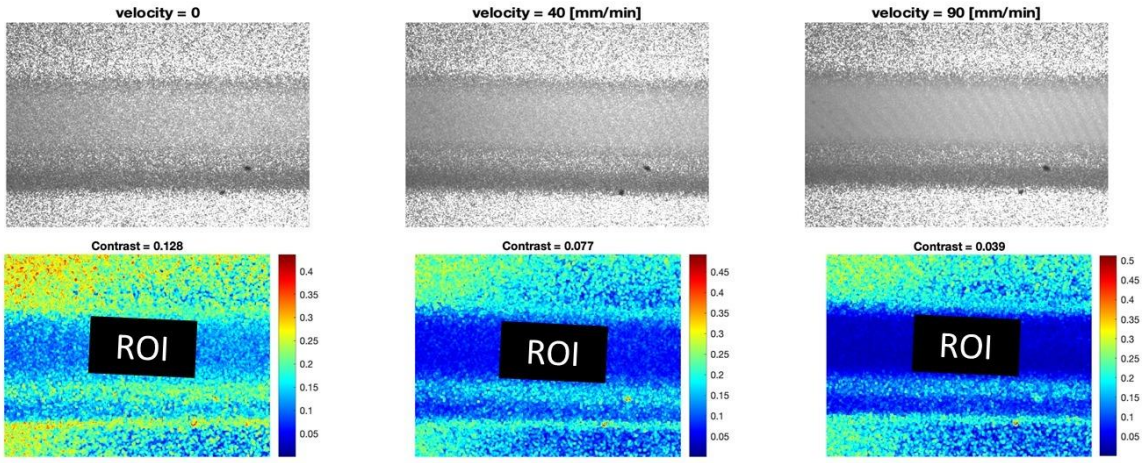

Figure 3

Conclusions: Speckle contrast techniques demonstrated its efficiency as a non-invasive real time tool for measuring tissue perfusion in our prototype. We have also proved that these techniques are sensitive for very small changes in particle velocity and allow to observe physical phenomena like velocity profile of a fluid or Brownian motion. Future work can be done to enhance image quality, to improve the ability to visualize deep blood vessels using principal component analysis and Kurtosis analysis.

Keywords: speckle phenomenon, tissue perfusion, laser speckle contrast imaging

(23)

Compact spectrally encoded interferometry probe for imaging acoustic vibrations in the tympanic membrane

Lidan Fridman, Matan Hamra, Rotem Yacoby and Dvir Yelin

Biomedical Engineering Faculty, Technion - IIT, Haifa, Israel

Introduction: Diagnosing hearing problems requires assessment of the multiple factors involved in the mechanical transduction of sound into the inner ear. These tests are some of the most common diagnosis procedures in the world, considering that approximately 466 million people (over 5% of the world population) suffer from some sort of a disabling hearing loss. In most cases, early detection and intervention could significantly reduce the negative impact of hearing problems; in some types of conductive hearing loss such as otosclerosis and otitis media, preventive treatment may include prescription of various drugs that would eliminate the need for hearing aids or surgical intervention.Direct measurements of tympanic membrane movements has been demonstrated using Laser Doppler vibrometry, optical coherence tomography and stroboscopic holography; *in vivo* imaging with these techniques, however, may be challenging due to the relative complexity of their optical systems and their slow scanning speeds.By encoding a single lateral dimension with wavelength, spectrally encoded endoscopy allows high-resolution imaging through a single optical fiber using compact imaging probes. By adding low-coherence phase-sensitive spectral-domain interferometry, interferometric spectrally encoded endoscopy (ISEE) has been shown capable of high-speed imaging of nanometer-scale vibrations of the tympanic membrane in human subjects. In this project, we design a compact hand-held ISEE probe that includes all the necessary components for effective imaging of the tympanic membrane in patients, packed within an otoscope-like apparatus that is easy to hold and operate with a single hand. This device will be constructed and used for clinical experiments.

Methods: ISEE measures the spectral interference between a reference beam and spectrally encoded reflections from the target tissue. Under acoustic stimulations, the axial tissue motion induces wavelength-dependent phase shifts that are captured by the high-speed spectrometer. By slowly scanning the imaging line across the tissue, the full vibration pattern is recovered at high lateral resolution and nanometric axial sensitivity.

Results: A user-friendly interface was developed using Labview for managing data acquisition procedures, real-time data analysis and display, operator feedback for easy positioning of the imaging probe, and data saving and storage. A bench-top optical setups was used to test the optical channels using off-the-shelf optical and optomechanical components. The compact optomechanical design was iteratively improved using Solidworks, and a detailed optical

simulation using Zemax was used to evaluate key imaging parameters such as resolution, field of view and optical aberrations.

Conclusions: A complete optical system was designed for *in vivo* imaging of the human tympanic membrane in patients, including a compact optical setup, optomechanical packaging, user friendly software and data acquisition hardware. Future work will include the manufacturing and assembly of the system, followed by optical characterization and feasibility tests in human volunteers.

Keywords: interferometric spectrally encoded endoscopy (ISEE), tympanic membrane, hearing problems, clinical diagnosis

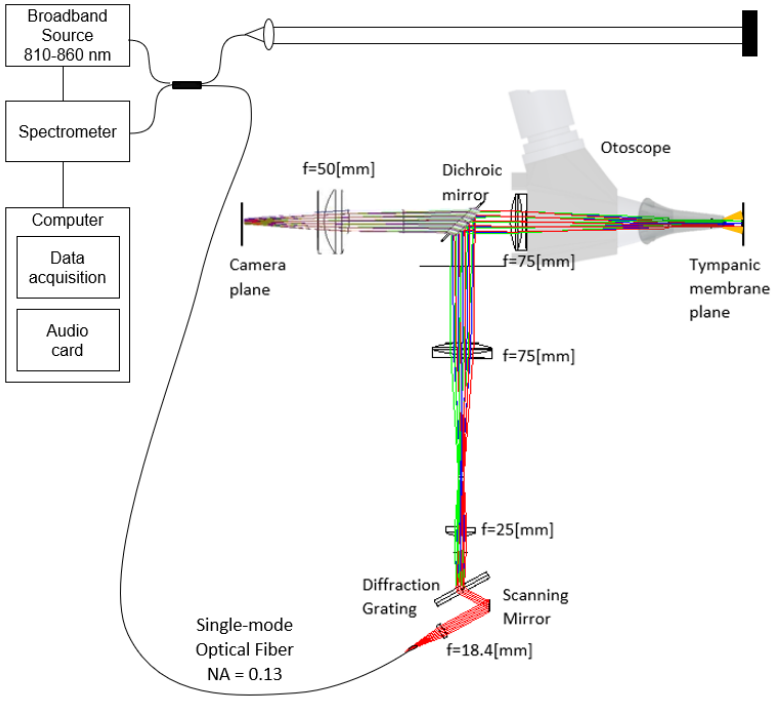

ISEE system integrated to a standard otoscope.

Figure 1

(24)

A Low-Cost 3D Printed Prosthetic Hand for Transhumeral Amputations

Niv Rebhun[1], Sofia Rozenberg[1], Yair Herbst [2], Oscar Lichtenstein [1], Yoav Medan[3]

[1] Biomedical Engineering Faculty, Technion - IIT, Haifa, Israel
[2] Department of Mechanical Engineering, Technion - IIT, Haifa, Israel
[3] Haifa3D Co-Founder and Chairman, Visiting Scientist, Technion - IIT, Haifa, Israel

Introduction: According to estimations, up to the end of 2020 there will be about 2.2 million people with upper limb amputations across the US alone. The loss of an arm has a great impact on the quality of life and a good prosthesis can help improve it. Although there is a large selection of different types of prosthetics on the market, there appears to be still room for improvement. The aim of this project was to design a body powered and 3D printable prosthesis for Transhumeral amputations which answers the main problems of current models. Since most prostheses are very expensive and not suitable for growing children, making the prosthesis 3D printable and body powered lowers the price drastically, increases the availability and makes it easy to adjust.

Methods: 3D printing - FFF (fused filament fabrication) is a layer by layer printing method. The basis of the method is adding a 2D layer on top of another 2D layer to construct a 3D model. FFF is the most common method, from home printers to industrial ones.

Material - we chose for our design the polymer ABS (Acrylonitrile butadiene styrene). ABS has relatively high glass transition temperature which makes it impact resistant and tough. Additionally, ABS can be printed with a very high precision, a quality important for our design due to mechanisms that consists of small parts.

Mechanism - body powered and therefore does not rely on expensive and heavy electrical parts such as engine or butteries.

Design & simulations - SolidWorks.

Results: We designed two models, both have the ability to adjust the elbow angle and operate a terminal device. These functions are enabled by a cable mechanism connected to a harness. The first design is more suited for patients with low amputation sites whereas the second design is more suited for higher amputation sites Both designs underwent mechanical strengths and limitations tests to ensure their functionality and safety. The prosthesis we designed met the requirements we set at the beginning of the project: They weigh under 1 kg each and they are fully operable by the harness cable.

Conclusions: In this article, we show the feasibility of a fully 3D printed Transhumeral prosthesis, but there is still need for more clinical and physical testing to ensure the prosthesis safety and functionality. In order to accomplish the next step of the project there will be a need for several people to try using the prosthesis. In case of shortage in suitable patients, we developed an adapter especially for healthy test subjects.

Keywords: Transhumeral amputation; 3D printable prosthesis; Body powered prosthesis.

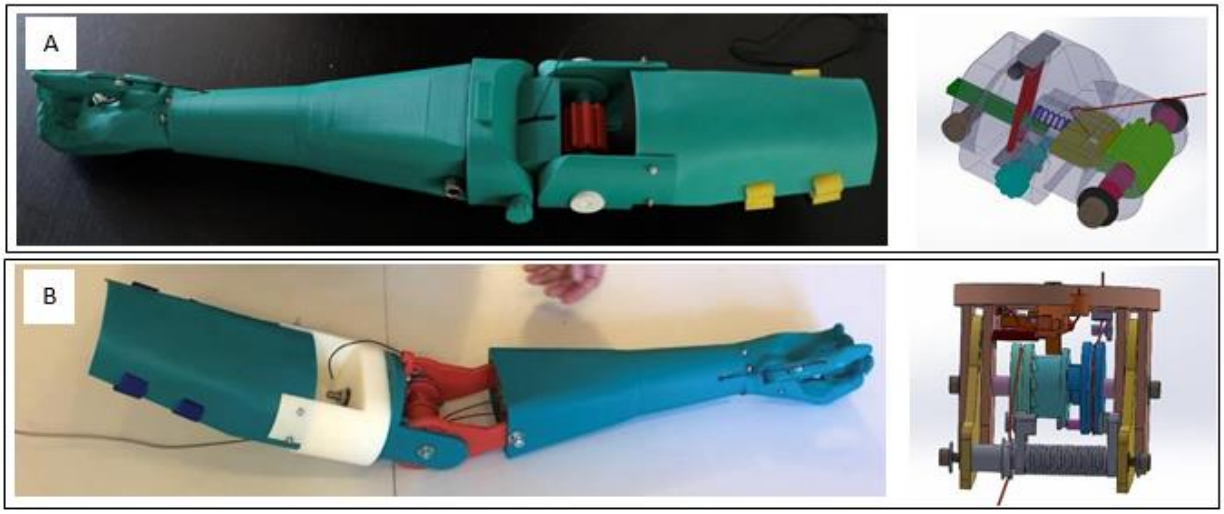

Figure 1: 3D printed functional models are on the left side, prosthesis mechanisms are on the right side. A- the first design -suitable for low amputation sites. B- the second design – suitable for higher amputation sites.

(25)

A Modular, Task Specific End Effector for A Low-Cost 3d Printed Prosthetic Hand

Ayala Goldstein[1], Yair Herbst[2], Oscar Lichtenstein[1], Yoav Medan[1]

[1] Department of Biomedical Engineering, Technion - IIT, Haifa, Israel
[2] Faculty of Mechanical Engineering, Technion – IIT, Haifa, Israel

Introduction: Around the world, there are many people with upper-limb amputations. Loss of an upper limb can be caused from many ~~and~~ ~~varied~~ reasons. Among other ~~things~~ reasons because of sickness, accidents, natural disaster or even from birth.The common solution to upper-limb amputations is a prosthesis which is very expensive and not always aesthetic or functional. To solve this problem, the global e-NABLE Community is using 3D printers to create 3D printed hands and arms for those in need. The 3D printed hand is much cheaper and also customisable. It is also possible to print end effectors that allows ~~you~~ to use the printed hand to perform a variety of operations. In this project I focused on design and development of a replacement accessory that will allow quick and easy replacement between end effectors.

Methods: To allow quick and simple replacement between the end effectors, I chose to design a replacement accessory that will always allow the prosthesis arm to be left attached, with the replacement being between the palm and the end accessories. This requires a detachment between the hand and the arm. I chose to design a replacement accessory with two lugs that fit into designated holes in the arm and disconnect by simply clicking on the accessory. The design is done by SolidWorks software.In addition, I planned and designed an end effector. I chose to design an accessory that allows cycling. Cycling is a recommended action for rehabilitation as well as for reintegration into society. I designed the accessory so that it connects to both the replacement accessory and the bike handlebars. To overcome safety issues the accessory is designed to automatically disconnect in a slight collision (up to 200 Newtons) and to automatically tighten in a severe collision (above 700 Newtons).

Results: The replacement accessory successfully withstood simulations performed in Solid software. The accessory was opened by pressing 1 Newton, according to the reasonable force of a human hand, and did not detach even under vibrations and external pressure.The cycling end effector properly disconnected and tightened under pressure. Unfortunately, refraction and tightening are not yet done regularly under the appropriate pressures, and the critical pressures vary depending on the angle of impact. It is likely that choosing different media will yield more accurate results.

Conclusion: In conclusion, both the replacement accessory and the end accessory met the simulation requirements we set for them. Hopefully in the future we will also be able to check their integrity and activity in field trials as well

Keywords: Prosthesis, end effector, replacement accessory, 3D printing.

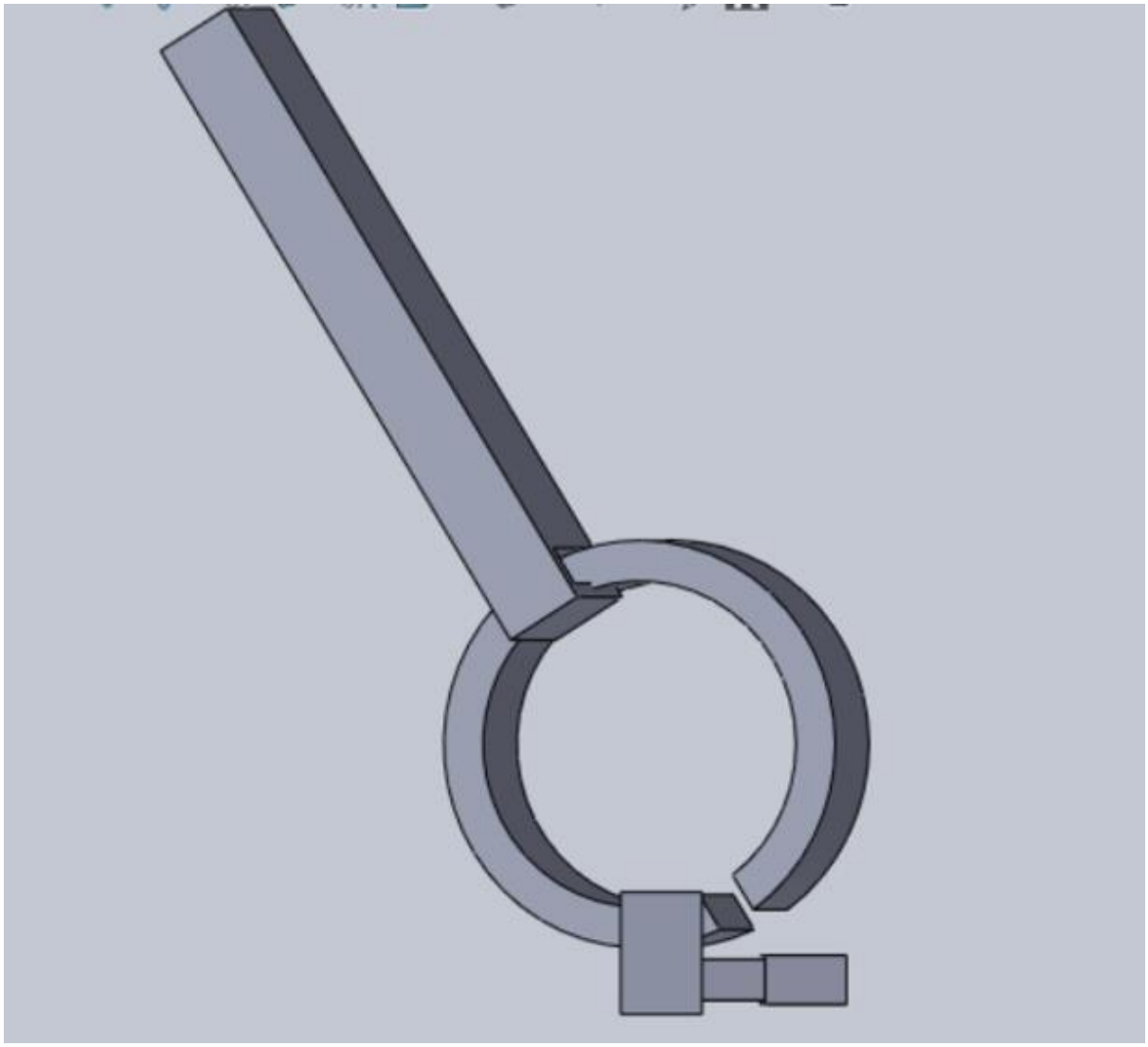

Figure 1- The cycling end effector.

(26)

Fully Automatic Adjustable CAD Model of a Wrist Powered, Low- cost, 3D Printed Prosthetic Hand

Mark Kels[1], Yair Herbst[2,3], Oscar Lichtenstein[1], Yoav Medan[3]

[1] Department of Biomedical Engineering, Technion - IIT, Haifa, Israel
[2] Faculty of Mechanical Engineering, Technion – IIT, Haifa, Israel
[3] Haifa3D, Haifa, Israel.

Introduction: Prosthetic hands are not readily available for all amputees, mainly due to the high cost of a prosthetic limb, which is amplified in cases where a new prosthesis is required often, usually due to a change in size. 3D printed prosthesis are a good low-cost solution, but currently require skilled personal in order to resize and adjust them in a patient-specific manner, thus resulting in a relatively complicated design process and/or a poorly fitted hand. Automatically adjustable CAD model, which requires only a limited skill level to use, may allow lay users to create 3D printed, low-cost, prosthetic hands.

Methods: A CAD model was created using Solidworks, in a manner that is suitable for automatic adjustment, i.e. variables, design tables and equations. In addition, a user interface for measurements input was created using MATLAB and AppDesigner. Measurements entered by the user are processed using the MATLAB app to convert anatomical measurements into parameters that are required by the CAD model. The CAD model is then automatically updated. The resulting model is compatible with 3D printing using various materials and with as low as 1mm resolution.

Results: A resulting model can be used for quickly adjusting a wrist powered prosthetic hand that is printable using a common 3D printer, by a user with very basic level of training in CAD. The user is required to measure seven anatomical parameters and enter them in a simple app, and the CAD model is adjusted accordingly.

Conclusions: Although the resulting prosthesis is limited in the variety of applications, sizes and quality of required printing capability, it might be a suitable solution for certain individuals with amputations with a functional wrist.

Keywords: Solidworks, 3D Printing, Prosthesis, Automatically Adjustable

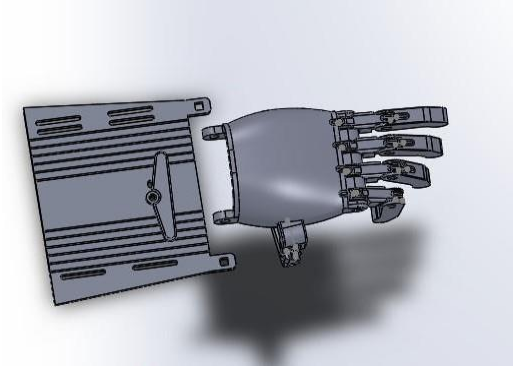

Figure 1: An assembly of automatically adjusted parts for a 3D printed wrist powered prosthesis.

(27)

Effect of Drag Reducing Polymers (DRPs) on Recirculation and the Deposition of Targeted Nano-Carrier in Human Arterial Models

Neta Tuaf, Oscar Lichtenstein, Maria Khoury, Netanel Korin

Department of Biomedical Engineering, Technion - IIT, Haifa, Israel

Introduction: Atherosclerosis is a cardiovascular disease in which the inside of an artery narrows due to the buildup of plaque. It is the underlying cause of 50% of deaths in the western world. Research have shown atherosclerotic regions are characterized by abnormal flow pattern that includes the formation of slow recirculation and low wall shear. In addition, it was shown that recirculation contributes to the formation of plaque and the progression of the disease.
Drag reducing polymers (DRPs) are a class of polymers that are characterized by their ability to reduce the frictional resistance to flow in pipes. Research have revealed that DRPs reduce the formation of plaque in *in vivo* animal models, however, the reason for that is still unknown. One of the hypotheses is that DRPs increase the shear stress in these areas, thus reducing the recirculation and the progression of the plaque.
In this work, our goal was to understand the effects of DRPs on particles deposition of drug delivering particles to disease site, i.e., the recirculation region.

Methods: 3D straight macro-channels were fabricated using PDMS. Endothelial cells were cultured inside the channels. A perfusion system which included a peristatic pump was used. For each experiment, the solution was perfused through the channel at a controlled constant rate to achieve physiological forces inside the channels of about 15 dynes/cm^2. The solution was perfused for 60 min in each experiment.
To assess the shear forces inside our models, we used $2\mu m$ fluorescent carboxylated polystyrene nanoparticles. Particle adhesion was monitored via florescent confocal microscopy and the number of adhered particles was extracted using a custom analysis software (Matlab®) .

A PBS solution was used as a control and a solution of Poly(ethylene oxide) (PEO) was used as our DRP solution. The DRP solution was made in three different concentrations, to check the effect on the deposition. The lowest concentration had the approximate viscosity of water (μ_{water}~$0.89\ mPa \cdot s$), while the highest concentration had the approximate viscosity of 4 times the viscosity of water
(~$4 \cdot \mu_{water}$).

To examine the effect of shear stress, particles were perfused inside the channel under approximately 60 dyne/cm^2.

Results: For all three concentrations of PEO the number of counted particles was lower than number of counted particles in the control solution. For the lowest concentration, we noticed a 47% decrease in adhesion, while for the highest concentration, there was a decrease of 17% in adhesion. In addition, our results showed that the adhesion was increased by 7.5 when the shear stress was increased by 4 (Fig.1).

Conclusions: There is a clear interaction between the polymer and the particles. This interaction increases with the concentration of the polymer and the shear stress. We may conclude that the polymer caused less particles to adhere to the walls of the model.

Keywords: Atherosclerosis, DRPs, recirculation, particles deposition.

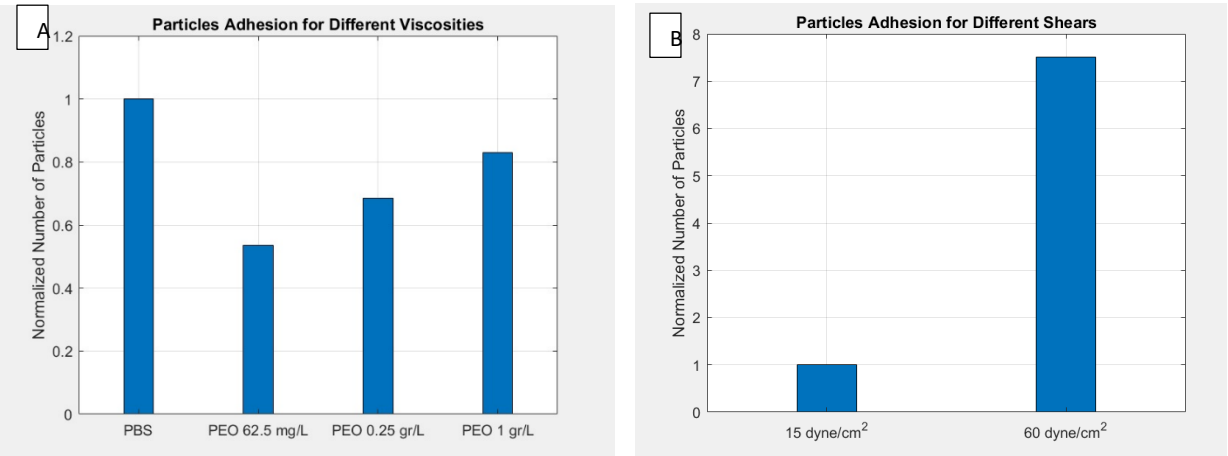

Figure.1: A) The effect of different viscosities on the particle adhesion. B) The effect of different shear stresses on the particle adhesion using the solution with the highest concentration of PEO.

(28)

Clot Fibrinolysis in CRAO Models Using Thrombolytic Therapy Triggered by Externally Low Intensity Ultrasound

Or Mizrahi, Omer Gottlieb, Moran Levi, and Netanel Korin

Department of Biomedical Engineering, Technion – IIT, Haifa, Israel

Introduction: The focus of our research is on the fibrinolysis of Central Retinal Artery Occlusion (CRAO) clots using thrombolytic therapy enhanced by low intensity ultrasound. To-date fibrinolysis of clots using thrombolytic therapy has been successful primarily in stroke patients. However, there is no standard treatment protocol for dissolving CRAO clots. Thus, our goal was to design and build CRAO models using thrombolytic therapy triggered by low intensity ultrasound excitation.

Method: The methodology we employ includes a combined experimental and numerical approach where the former is based on both ex-vivo and in-vitro models and the latter incorporate computational fluid dynamics (CFD) simulations using Ansys Fluent solver.

Results: Our main results are twofold: (i) an anatomically accurate microfluidic in-vitro Polydimethylsiloxane (PDMS) model was designed and built to yield clot dissolution in the presence of tissue Plasminogen Activator (tPA) and plasminogen (tPA is a protein involved in the breakdown of blood clots, catalyzes the conversion of plasminogen to plasmin, the major enzyme responsible for clot breakdown) . We made use of a standard clot (comprised of platelets, fibrin and red blood cells) and a fibrin clot where the latter required a larger amount (x10) of tPA for complete dissolution. Ultrasound excitation of a static clot model injected with tPA droplets revealed faster dissolution of the clot than a static clot model injected with only tPA droplets (ii) a CFD model incorporating identical geometry and fluid properties to those of the in-vitro model revealed both flow velocity increase (200%) and an order-of-magnitude increase of wall shear stress at the clot location. Emulation of blood clot shrinkage by an ice particle subject to heat transfer demonstrates flow streamlines and evolution of wall shear stress during the dissolution process.

Conclusions: The main conclusions of this research are that clot fibrinolysis of an experimental in-vitro CRAO model using thrombolytic therapy with ultrasound excitation is a viable methodology for clot dissolution, and that a CFD based investigation can be employed for optimal process design. We expect that low intensity ultrasound excitation will enhance clot dissolution with a small amount of tPA. Future research will investigate a CRAO ex-vivo model using porcine eyes to validate the results of the in-vitro and CFD simulations.

Keywords: Thrombolytic therapy, Fibrinolysis, Clots.

Vocal Vibes

(29)

Remote Speech Therapy technology

Marina Tulchinsky[1], Roni Keshet[1], Ori Shahar[1], Shaked Ron[2], Oscar Lichtenstein[1]

[1]Department of Biomedical Engineering, Technion - IIT, Haifa, Israel
[2]Department of Medicine, Technion - IIT, Haifa, Israel

Introduction: 7.7% of U.S. children suffer from voice and throat related disorders, also 7.6% of adults (over 18) report having some speech problems in the last year. It has been shown that working with a speech therapist in a Voice Therapy Program can improve speech disorders such as behavioral dysphonia. An average of 14 million are working with a speech therapist in a year in the USA. Due to the COVID19 pandemic, many elective treatments such as speech therapy had to change to remote treatment in order to keep quarantine and to lower the risk of exposure. Remote sessions need to overcome the difficulty to assess the performance of the patient indirectly, our project aims to improve the ability to track the performance of patients during self-practice or remote sessions as well as helping with objective diagnosis using different methods such as: image processing, voice analysis and piezoelectric signal processing.

Methods: we use "DeepLabCut", a marker-less tracking algorithm to monitor the movement of the lips and mouth area, and MATLAB program to find the relative movement of each section of the mouth. We implemented a PCA-based classifier capable of recognizing bad speaking habits of the patient for two different exercises commonly used in speech therapy. As shown in graph A, we demonstrate a unique capability to determine sessions of exercises that are wrongly performed 100% sensitivity* (n=2 people).

We used the Saarbrucken voice database to test for the ability to identify patients with dysphonia using voice only during one exercise. Graph B shows the test and the classifying mark, we reached 91% sensitivity*(n=200 people, half dysphonic and half healthy).

We used piezoelectric sensors to differentiate "s" sound and "z" sound, those sounds are used for exercises commonly done during a speech therapy and was harder to differentiate using microphone only. Graph C shows the test and the classifying mark, we reached 88% sensitivity* (n=3 people).

Results: all classifiers are presented in figure 1. We reached sensitivity of 100% in the "U" exercise, using only the image processing tool. We reached sensitivity of 91% in the "E" exercise, using only the microphone database. We reached sensitivity of 88% in the "S/Z" exercise, using the piezo-electric sensor alone.

Conclusions: the results show that our aim to make remote assessment of speech performance an applicative tool is feasible. We assume that with a combination of all three methods we should achieve even better results that will change the speech therapy world in diagnostic and remote therapy aspect and bring it to the 21st century.

Keywords: deep learning, image processing, speech therapy, remote medicine

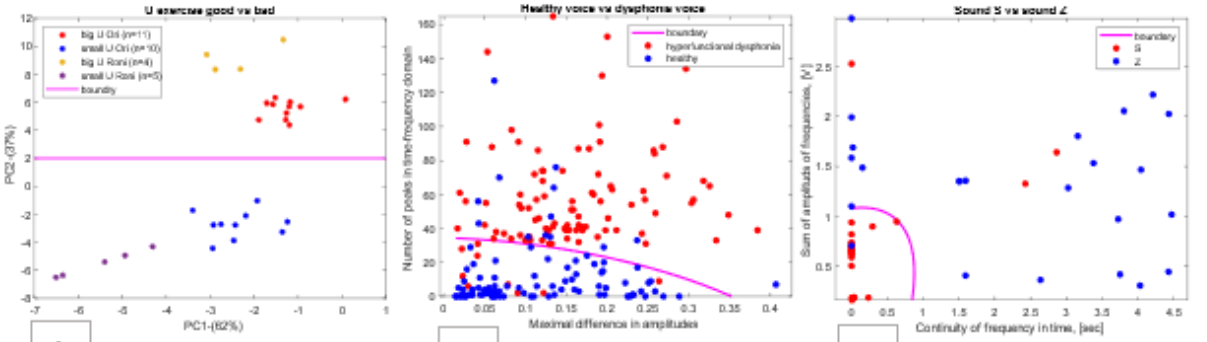

A

	Predictive positive	Predictive negative
Actual positive	TP = 15	FN = 0
Actual negative	FP = 0	TN =15

B

	Predictive positive	Predictive negative
Actual positive	TP = 91	FN = 9
Actual negative	FP = 12	TN =88

C

	Predictive positive	Predictive negative
Actual positive	TP = 23	FN = 1
Actual negative	FP = 3	TN =21

Figure 4: A- image analysis differentiating correct and incorrect "U" exercise | B- sound analysis diagnosis for Dysphonia | C- piezoelectric analysis to find "s" sound vs. "z" sound| In the tables are the statistic row data.

(30)

Optimization of Dual Drug Co-Encapsulation in Cancer Targeted Nanoparticles

Amjad Marie, Sanaa Dallashi, Dana Azagury, Arbel Artzy-Schnirman, Yosi Shamay

Department of Biomedical Engineering, Technion- IIT, Haifa, Israel

Introduction: Anti-Cancer drugs, with different mechanisms, are most effective when given in combination, reducing chances of cancer cells developing resistance to the treatment. However, administrating a combination of drugs can cause a significant increase in side effects, especially considering the common drug delivery systems. According to recent studies, nanoparticles can serve as a system for delivering a high dose of drugs directly to cancer tissues with minimal effect on healthy cells, thus, reducing the side effects. Preparation of drug-loaded nanoparticles is a process based mainly on trial and error which makes it difficult to predict the outcome. Previous studies have successfully created a prediction model that predicts the product of NPs (nanoparticles) preparation method called nanoprecipitation for single drug loaded NPs. Our main goal in this project is to produce and characterize nanoparticles containing two different anti-cancer drugs in order to create a database for a future prediction model.

Methods: Nanoprecipitation - We add 150 μL of a single or combined drugs dissolved in DMSO (10 mg/mL) to a solution of 50ml sodium bicarbonate (0.1M) with 100μL of selected dye (2mg/mL). The solution is then centrifuged (30,000 rpm, 15 minutes) and the pellet is re-suspended in 1 mL DDW. We produced and characterized 16 single drug-loaded NPs by measuring their mean size and its poly-dispersity index (PDI) using dynamic light scattering (DLS) and divided them into 4 main categories: (1) Drugs that form “good” long term stable nanoparticles (2) Drugs that form “good” short term stable nanoparticles (3) Drugs that form “Bad” (>150nm, too big) NPs (4) Drugs that do not form any NPs (<5nm, too small). Next, we decided to produce combinations of dual drug NPs. In each combination we selected one drug from the first category and the other from the other categories. Then we characterized the combinations’ mean size and PDI to label the stability status and also quantified the amount of drugs encapsulated in NPs and evaluated the encapsulation efficiency via HPLC.

Results: In at least 9 out of 17 Nanoparticles that were produced by Nanoprecipitation with two drugs, the NPs were stable and contained both drugs, including NP combinations with drugs that previously failed to nanoprecipitate as single drugs. In addition, in cases in which two different NP combinations with the same unstable drug, but with different stable drugs used, had significantly different results. One combination was stable and the other was unstable. We also

used different kind of stabilizer called IR-820 to see its effect on two combinations that were unstable when we used the original stabilizer IR-783, and it succeeded to stabilize both combinations.

Conclusions: Generally, stable drugs can help stabilize unstable drugs. Different stable drugs may differ in their ability to stabilize a specific unstable drug. In addition, we have succeeded in containing a non-precipitated drug, in a stable NP. While IR783 has failed to stabilize some drug combinations, different stabilizers may be used in order to stabilize the same drug combinations. The data we collected will be used in a future model to predict dual drug Nanoprecipitation.

Keywords: cancer drug-delivery system, nanoparticles, nanoprecipitation, drug combinations, prediction model

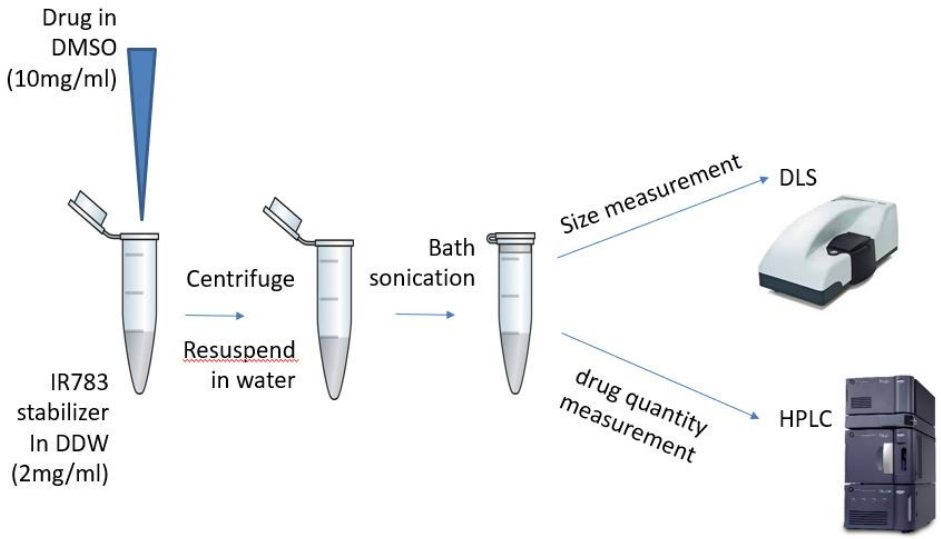

Figure 1: Schematic illustration of drug-loaded nanoparticle preparation with Nanoprecipitation method.

(31)

Increased Extracellular Vesicle (EV) Production From 3D Engineered Skeletal Muscle Tissue Under Mechanical Stretching

Tahel Carmon, Adina Israel Fried, Lior Debbi, Shaowei Guo, Arbel Artzy-Schnirman, Shulamit Levenberg

Biomedical Engineering Faculty, Technion IIT

Introduction:Skeletal muscle regeneration in the body is limited. Although it can regenerate after minor injuries, major injuries can result in irreversible damage to skeletal muscle, leading to scarring, fibrosis and even loss of muscle function. The current mainstay solution for repairing scarred tissue is reconstructive surgery. However, this approach is invasive and fails to address critical requirements for clinical use. The research presented here is part of a larger study in using extra-cellular vesicles (EVs) as a non-invasive approach to encourage muscle tissue regeneration after acute injuries. Specifically, this study investigates the ability to enhance EV production by mechanical stimulation of an engineered muscle construct cultivated on a 3D elastic scaffold with defined orientation.

Methods:A directional matrix scaffold was first fabricated using 3D printing techniques, based on polydimethylsiloxane (PDMS) polymer, to maximize cell infiltration and encourage cell alignment. The mechanical properties were tested using the Bose Intron system to confirm scaffold resilience in a physiological stretching profile. Mature skeletal muscle tissue was then engineered by seeding the scaffolds with myoblasts and promoting differentiation into aligned myotubes. When the muscle cells matured, the scaffolds were cyclically stretched for 48 hours in a bioreactor (25% at 1 Hz) and compared to a control group under static conditions. EVs from both stretched and unstretched scaffolds were then harvested and characterized using ultracentrifuge and Nanosight technology, respectively.

Results:Myoblasts on directional matrix scaffolds were successfully able to mature into aligned myotubes after 21 days of culturing, as shown through Desmin immunofluorescence staining. In addition, EVs from the stretched scaffolds were significantly higher in concentration than the unstretched controls, suggesting that myotubes in stretched scaffolds are able to sense mechanical stresses and respond accordingly through the release of additional EVs. This mechano-sensing was confirmed through the comparison of Yes-Associated Protein (YAP) concentrations in the nuclei between stretched and unstretched scaffolds.

Conclusions: Induced stretching on engineered skeletal muscle promotes the increased release of EVs in order to initiate muscle healing. This finding could be the foundation for enabling muscle recovery through the induction of intensive natural muscle repair through infusion or direct injection of extracellular vesicles. On a larger scale, this groundwork can be used as a steppingstone for future research in the reconstruction of all types of muscle, including minimally regenerative cardiac tissue.

Keywords: Skeletal muscle regeneration; extracellular vesicles; cyclic stretching; 3D elastic scaffold

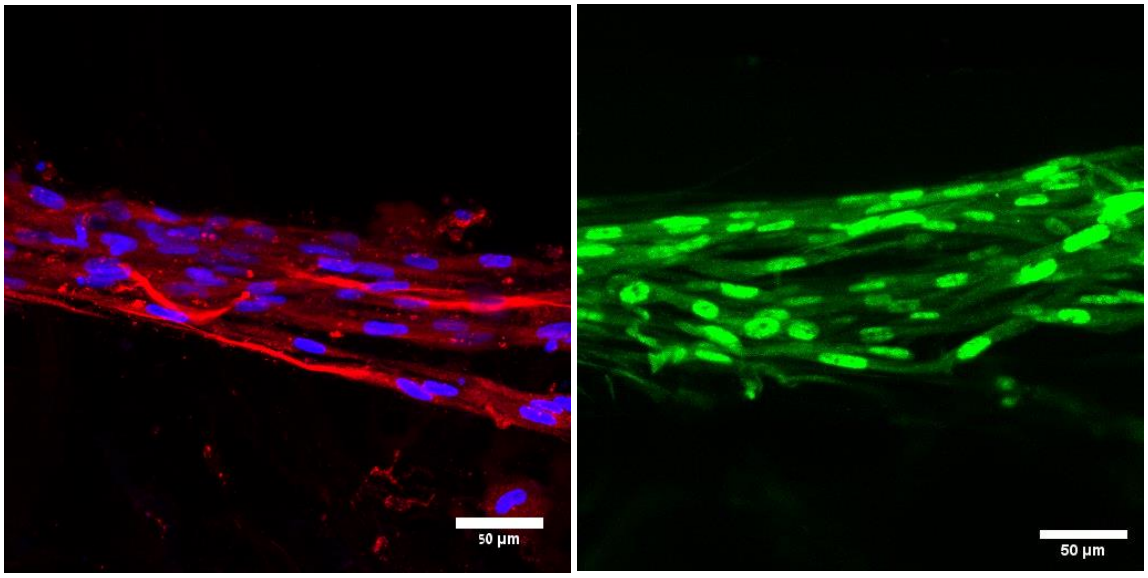

(A) (B)

Figure 1: Immunofluorescent staining of stretched scaffolds to confirm engineered skeletal muscle maturation and test mechano-sensing of myotubes

(A) ***Staining with DAPI (blue) and Desmin (red) to show myotube maturation and alignment***

(B) ***Staining with YAP (green) to verify mechanotransduction of cells***

BME Biomedical Engineering TECHNION Israel Institute of Technology

(32)

The effects of natural remedies on the invasiveness of metastatic cancer cells

Stav Elkabetz, Sally Kortam, Arbel Artzy-Schnirman and Daphne Weihs

Department of Biomedical Engineering, Technion - IIT, Haifa, Israel

Introduction: Cancer is one of the deadliest diseases globally and the leading cause of death is cancer metastasis. These days, the alternative treatments are accelerating, although its application is not fully understood. The natural remedies that we will discuss are Curcumin and Fenugreek. There are many reports that curcumin have medical benefits; anti-infectious, antioxidant, anti-inflammatory, hepatoprotective, cardioprotective, thrombo-suppressive, and anti-arthritic. The anti-cancer effects of curcumin are mediated mainly through its negative regulation of various transcription factors, growth factors, inflammatory cytokines, protein kinases, and other oncogenic molecules. Fenugreek is a herb from the Leguminosae family and it's seeds are used for its medicinal properties. Fenugreek has been used for centuries as a remedy for different disorders, such as diabetes, inflammation, wounds, and high cholesterol. In recent research, fenugreek seeds were experimentally shown to have anticancer potential against various cancer cell lines. The main goal of the project is to examine the effects of natural remedies, fenugreek and curcumin, on the metastatic potential and mechanical invasiveness of cancer cells. Therefore, performing a comprehensive Literature review on the extraction process methods for future work.

Methods: We will examine our hypothesis using the mechanobiology-based assay developed by the Weihs research group. First, preparation of polyacrylamide gel within the tissue physiological range, using the rheometer for determining the stiffness of the gel. Simultaneously, the cancer cell line culture was gown, using AsPC-1 cells, a highly metastatic pancreatic cancer cells driven from human ascites. We focused on the Extraction process of the active ingredients from the plants, via various methods, this way understanding the advantages and disadvantages of each method. At the end of the project, we executed the experiment using a fluorescence microscope and analyze the results.

Results: We developed a viability test protocol that will be the foundation of future experiments. The viability test aims to examine the influence of the plants on the cancer cells and determine the right concentration of the extract. As a part of assembling the protocol, we performed a comprehensive literature review on the extraction process and the different aspects of each method. Then, according to the literature review, we decided on the best method for concentration and extraction of the plant, that we will, later on, see its impact on the cancer cells.

In order to extract the plant, it is necessary to be sure that the concentration of the extraction is satisfying. To do so, we used two methods: The first was pH test with comparison to neutral pH. The second was an analysis of the amount of absorption of the light via spectrophotography to quantification the plants extraction. We used a water solution and measured the light absorbed at 370 nm and 420 nm. (for curcumin and fenugreek, respectively, and according to the fluorescent activity of the plants obtained from the literature).

Conclusions: From the literature, there is some real evidence that natural remedies, especially fenugreek and curcumin can be therapeutic in cases of cancer. Prior to the experiments, it is crucial to fully understand the different methods of extraction of each plant, and their special properties.

Keywords: curcumin, fenugreek, cancer, natural remedies

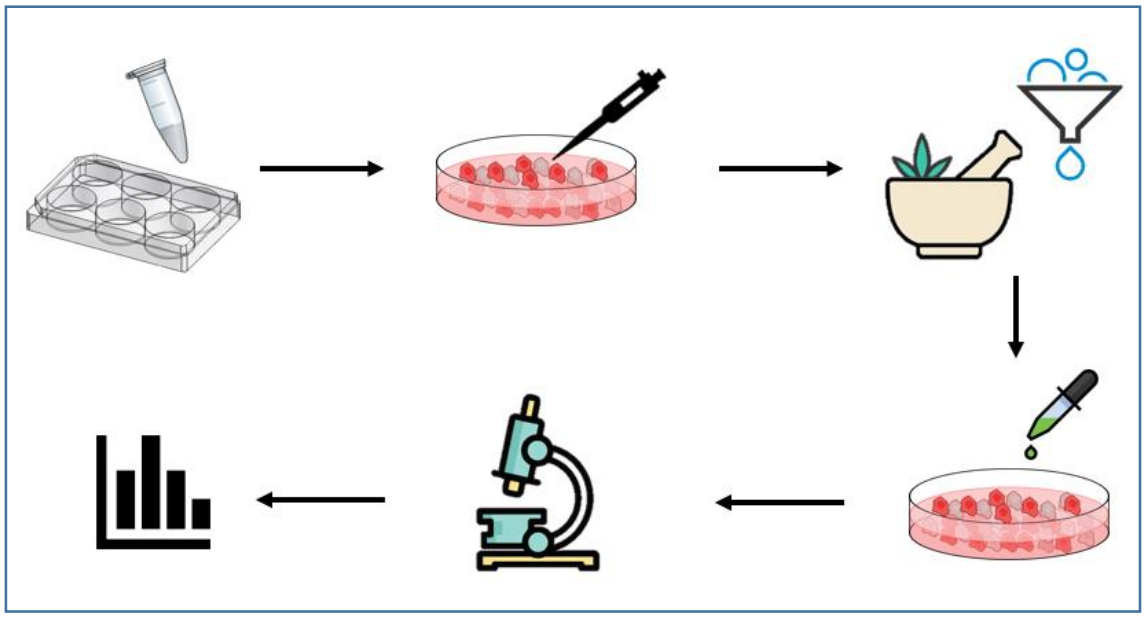

Figure 1: The project process. From the extraction of the remedies and the treatment of the cancer cells, the preparation of the polyacrylamide gel to the operation of the experiment.

(33)

Developing an Optimized Method for Efficient Automated Nano-Particles Preparation and Characterization

Yarden Roth, Maytal Avrashami, Yuval Harris, Arbel Artzi-Shnirman, Yosi Shamay

Department of Biomedical Engineering, Technion - IIT, Haifa, Israel

Introduction: Nanomedicine is a research field that applies the knowledge and tools of nanotechnology to the prevention and treatment of disease. According to the Enhanced Permeability and Retention Effect (EPR), nano-particles (NPs) tend to accumulate in tumor tissue due to their small size that enables them to pass through holes in the cancer's imperfect blood vessels. Recent discoveries in the Shamay Lab introduce self-assemble NPs that are composed of cancer drug particles and stabilizer particles solely. Developing an automated method to prepare these NPs will enable a more efficient research and more reliable results.

Methods: Manual preparation of NPs was necessary to understand the wanted results and to compare the robot-made NPs to. To accomplish the automation goal, I designed a custom made 15 ml tube holder using SolidWorks and printed it on a 3D printer. This tube holder was successfully read by the Andrew Alliance liquid handling robot for executing protocols. It fits our need to clean particles using PD10 size exclusion chromatography in an automated protocol, and offers larger capacity for mass production of NPs. The first protocol I designed in the Andrew Alliance software was intended to test the optimal drug addition height to the test tube using the robot's pipettes and at the same time, test the optimal pipetting speed for mixing the solution. In this protocol I used Sorafenib drug and IR- 820 stabilizer. Iterations of this protocol were needed to improve the protocol design and repetitions of that protocol were performed to get consistent results. I evaluated my data using High Pressure Liquid Chromatography (HPLC) for characterization of the particles, by estimating the drug concentration. Dynamic Light Scattering (DLS) was used for quantification of the particles, by assessing their size and quantity in a sample. Analyzing these results was according to predetermined parameters and limits such as particle size smaller than 150 nm, Polydispersity Index (PDI) of a sample, which describes the width of the

assumed Gaussian distribution of particle size, less than 0.25, and the drug percentage of the sample close to 80% drug. The second protocol I designed, based on the results of the first, tested new combinations of drugs with stabilizers for NPs preparation. I tested Erlotinib, Alpelisib, Carlotimib and Trametinib drugs with potential stabilizers IR-820 and Albumin.

Results: The size of robot-made NPs was 79 nm and the size of manual-made NPs was 55 nm. The results of the first protocol provided a range of drug percentage between 78.9% and 87.7%, particle size range of 60.49 nm to 82.2 nm, and PDI range of 0.110 to 0.139. Therefore, all results were withing limits. The chosen height is the lowest one, inside the solution, and the chosen pipetting speed is the fastest speed option .The results of the second protocol yield that the drugs Carlotimib and Trametinib self-assemble with stabilizer IR-820 to form NPs, and that Albumin is a bad stabilizer as it did not self- assemble with any of the drugs.

Conclusions: Recent NP preparation automation work yield great results within the predetermined limits. It proves to be efficient but can be improved in future work to provide automation of the whole process from end-to-end.

Keywords:nano-particles, automation, self assemble

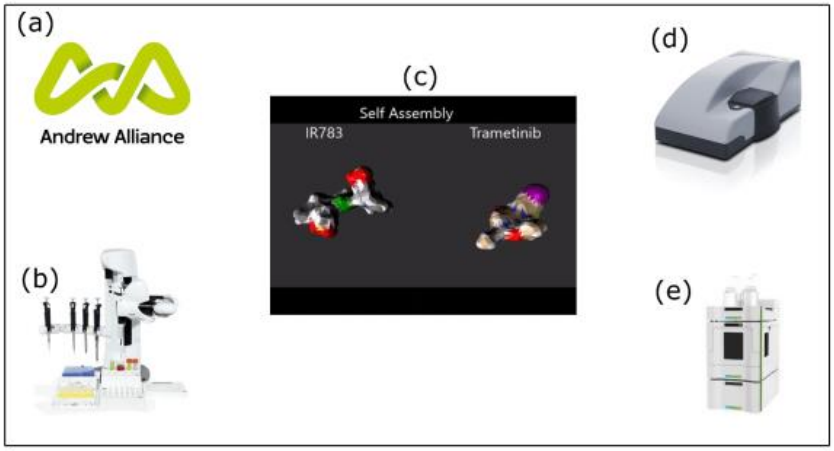

Figure 1: Protocol Planning and Execution Iterations. (a) planning protocols on Andrew Alliance software (b) executing protocols on Andrew robot (c) self assembly illustration of drug (Trametinib) with stabilizer (IR-783)(d) evaluation of results using DLS (e) evaluation of results using HPLC.

(34)

Wearable Diagnostic Patch for Monitoring Health Status

Nadi Hathot[1], Jalil Bishara[1], Youbin Zheng[2], Arbel Arzy-Schnirman[1], Hossam Haick[2]

[1]Faculty of Biomedical Engineering, Technion IIT
[2]Faculty of Chemical Engineering, Technion IIT

Introduction: As people age, the risk of developing multiple diseases increases, and the need for various checkups grows. Therefore, developing a sensor which can monitor multiple biomarkers in real-time, which indicate the presence of various diseases, will greatly protect the patient's well-being. Conventional checkup methods employ blood tests to gather data on a specific biomarker; these invasive and minimally-invasive methods might lead to infections if not done correctly. Hence, it is safer and easier to use a non-invasive sensor.

Herein, we seek to develop a non-invasive flexible FET-based biosensor that uses body sweat to monitor biomarkers. And as a proof of concept, we developed a duo-sensor for pH and Glucose monitoring.

Methods: we designed two models for the sensors: the first is based on silver nanowires synthesized in the lab, and the second is based on gold electrodes. We spray-coated silver nanowires onto a laser-cut model of the electrodes and the extended gates that is placed on a silicon wafer. Then we coated the electrodes with a flexible polymer using a spin coater. Afterwards, we peeled the silicon wafer to get a flexible sensor. with the second model we used electrode beam evaporation to deposit the gold onto the template. Carbon black layer was sprayed using a spray gun onto the extended gates. For the pH sensor we modified the extended gate using either poly(styrene-co-methacrylic acid) (PSMA) drop-casting or electrochemical deposition to deposit Polyaniline (PANI). Whereas with Glucose sensor we used the same method to deposit Prussian Blue, following that we drop-casted Glucose oxidase enzyme (GOx) and placed it under vacuum overnight.

The testing of the sensor's viability was done using a system based on a LabView program present in the lab. We then checked the sensor's response to various Glucose and pH concentrations and monitored the changes in the transistor's current (I_{ds}).

Results: As seen in figure (1) the results showed a clear differentiation in I_{ds} values between different pH and Glucose concentrations which proves the Viability of the sensor.

Conclusions: from figure (1b) we can see that I_{ds} values change accordingly to the pH levels. which means that pH monitoring via this method is possible. On the other hand, in figure (1a) we can see the transfer curve shifting accordingly to different glucose concentration. The initial results

showed better differentiation using the gold sensor. However, more testing with different sensor modifications should prove similar results between silver and gold. These finding prove that biomarker monitoring from sweat is possible using an FET-based transistor. Thus, sensor expansion to other biomarkers is feasible.

Keywords: Field Effect Transistor (FET); non-invasive sensor; glucose oxidase (GOx); Polyaniline (PANI); poly(styrene-co-methacrylic acid) (PSMA).

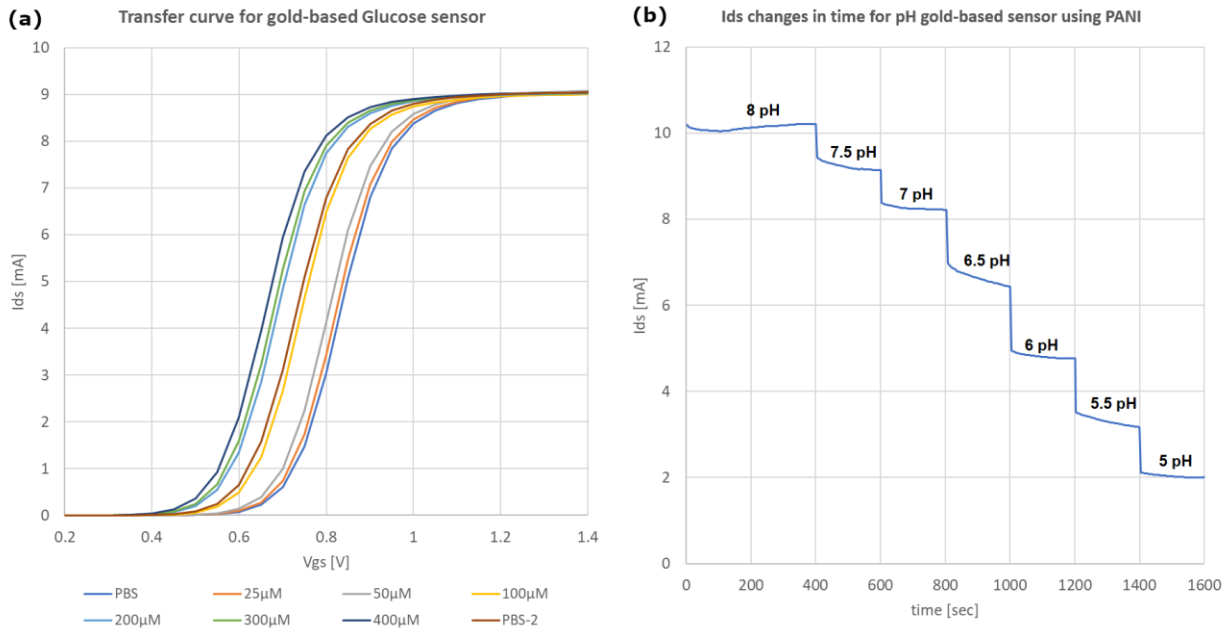

Figure 5: representative graphs, (a) transfer curve - Au Glucose, (b) Ids change - Au pH

BME Biomedical Engineering TECHNION Israel Institute of Technology

(35)

Effects of Cancer Conditioned Medium of High Metastatic Cells on The Invasive Behaviour of low-Metastatic Pancreatic Cancer Cells

Liubov Akselrod, Yulia Merkher, Sally Kortam, Daphne Weihs

Faculty of Biomedical Engineering, Technion IIT

Introduction: The main reason for cancer-related death is metastasis. In presence of high metastatic potential cells, the low metastatic potential cells may increase their metastatic ability. The influence evaluation can be investigated by Conditioned Media. Conditioned Media is growth media with various cell population secreted factors. Through a mechanobiology based assay, the mechanical invasiveness of conditioned medium treated low metastatic potential pancreatic cancer cells was evaluated.

Methods:

1. Polyacrylamide gels were prepared at physiological stiffness (Young's modulus of 2400 Pa), according to established protocol. The gels were covered with the collagen type I. Gel mechanics were evaluated with a rheometer.
2. Cell lines that were used in the research are AsPc1 as a high metastatic potential cell, and Panc1 as low metastatic potential cells. Cell lines were cultured in their appropriate RPMI-1640 medium, supplemented with bovine serum (FBS) and other supplements. Cells were cultured at 37 °C, 5% CO2, and high humidity. Viability staining was done by using Calcein-AM for viability staining and Hoechst for nuclei stain.
3. Conditioned Media from AsPc1 was collected after 24 hours of incubations and applied for 24 hours on Panc1 cell lines. It was decided to implement to types of assays: one consists of 100vol% Conditioned Media, and second consists of 50vol% Conditioned Media and 50vol% of Growth Media. 100vol% Growth Media was used as a control group in both cases.
4. We seeded stained 300K on each gel within the appropriate cell media.
5. The imaging was done with an inverted, epifluorescence microscope. Imaging was performed after 45 min of seeding. Using the custom microscope-control module in MATLAB, each field of view was scanned on few focal planes.
6. Images from the microscope were analyzed, and indentation depth, number of indenting cells and their viability were investigated.
7. To compare treated by Conditioned Media cells and by Growth Media control groups, as well as different CM types treatment groups, statistical analysis was provided.

Results: Using the mechanobiology based assay, we have evaluated the mechanical invasiveness of established Panc1 cells line incubated with Conditioned Media components of 50vol% (n=3) and 100vol% (n=3) and control group. For each of Conditioned Media experiments, a control group was performed. The averaged value of indentation depth for Conditioned Media 100vol% was 2.8 μm with mean value of indenting cells was 44%. The mean value of indentation depth for Conditioned Media 50vol% was 3.2 μm with mean value of indenting cells was 74%. Control group showed 2.2 μm mean value of indentation depth and 38% with mean value of indenting cells.

Conclusions: Conditioned medium of high metastatic potential pancreatic cancer cells was able to increase the invasiveness of low metastatic potential pancreatic cancer cells under specific parameters. The influence of surrounding of cancer cells on their mechanical invasiveness is a very important factor in metastatic development process. A better understanding of the interactions between cancer tumor cells and its environment might be a useful tool for cancer behavior prognosis and treatment decision process.

Keywords: Pancreatic cancer, Conditioned medium, Gel indentation assay, Metastatic potential, AsPc1, Panc1.

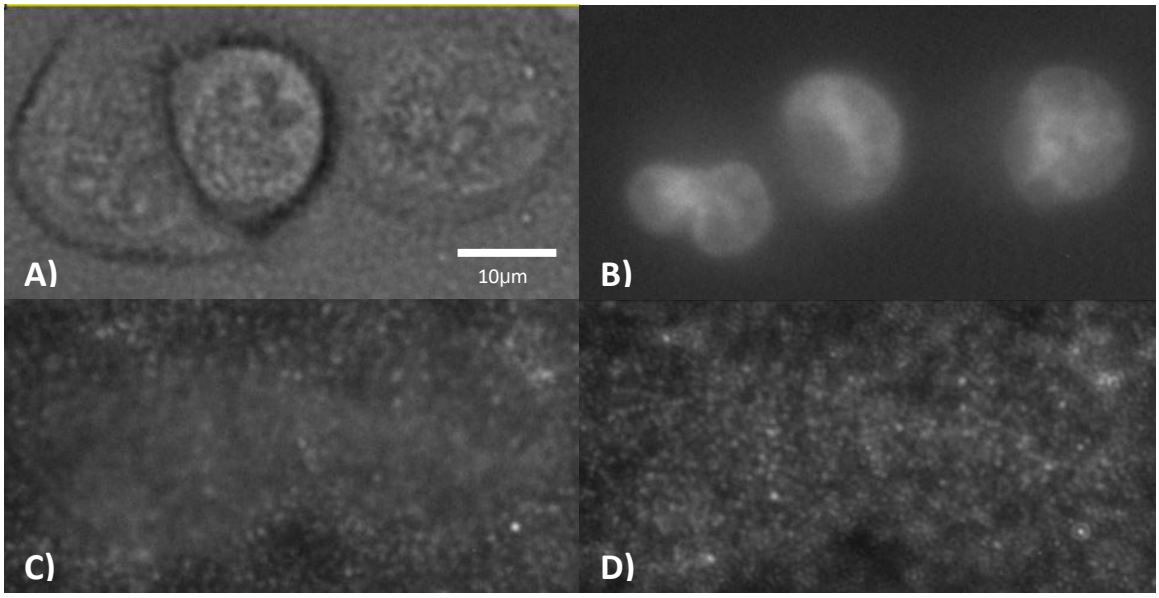

Figure 6: Panc1 in Conditioned Media from AsPc1 50% and Growth Media 50%.
A) DIC image of cell morphology
B) Hoechst nuclei staining image
C) Fluorescent image of particles at gel surface
D) Fluorescent image of particles moved to 3.3 μm depth below the gel surface by indenting cells

(36)

Recombinant p27 Liposomal Drug Intended to Inhibit the Uncontrolled Proliferation of Cancerous Cells

Maya Hershko[1,3], Danielle Sitry Shevah[3], Arbel Artzy Schnirman[1], Avi Schroder[1,2]

[1] Faculty of Biomedical Engineering, Technion IIT
[2] Faculty of Chemical Engineering, Technion IIT
[3] Faculty of Medicine, Technion IIT

Introduction: Cancer remains one of the most prevalent diseases, with an estimate of two million new cases and half a million deaths in 2020. Current cancer treatments include surgical intervention, radiation and chemotherapeutic drugs which often also kill healthy cells and cause toxicity to the patient. Therefore, it is desirable to develop drugs that can specifically target cancerous cells and decrease collateral damage to healthy tissue. In this study I worked to develop a nanoparticulate liposomal drug delivery system that targets cancerous cells and supplies them with non-degradable p27 protein. p27 is a nuclear protein that serves as a negative regulator of cell division. It has been shown that levels of p27 are low in many types of aggressive cancers, due to rapid degradation. It follows that introduction of recombinant non-degradable p27 into cancer cells may inhibit the uncontrolled proliferation of such cells, and thus prevent the rapid progression of the cancerous disease.

Methods: I produced a recombinant mutant of protein p27 which is an active cell inhibitor that cannot be targeted for degradation. The function of the recombinant p27 was estimated by a custom radioactive function assay I created, which examines the proteins ability to inhibit the kinase activity of Cdk2/Cyclin-A. Then the recombinant p27 was incorporated into ~100nm liposomes via Ethanol Injection and introduced onto cancerous cultured cells. The same methods were used to create empty liposomes that were also introduced to cancerous cells and served as negative control.

Results: The cultured cancerous cells treated with p27 liposomes did not show substantial decrease in proliferation in comparison to the cultured cancerous cells treated with empty liposomes. Quantification of p27 protein in the treated cells revealed that the amount of the exogenous recombinant p27 exceeded that of the endogenous p27 by ~85-fold. The location of the liposomes and recombinant p27 protein in the treated cells was examined by confocal microscopy. The confocal images indicated that the liposomes entered the cells via endocytosis, what would later cause their degradation in the lysosome. These results implied that the lack of inhibition in the treated cells was not caused by inadequate transportation of the recombinant p27

into the cells, but rather due to the liposomal uptake mechanism and the digestion of the recombinant p27 protein in the cellular lysosomes.

Conclusions: Development of a liposomal drug delivery system that targets cancerous cells and supplies them with non-degradable p27 may be possible. At this time, I have managed to create a functional non-degradable recombinant p27 protein and incapsulate it in liposomes. However, these liposomes seem to enter the cancerous cells via endocytosis which causes the degradation of their content. Currently I am working on adjusting the drug delivery system such that the liposomes will enter the cells by fusion and the recombinant p27 will be delivered into the cytoplasm of the cancerous cells. The recombinant p27 protein has a nuclear localization signal and will thus be transported into the nuclease where it can perform its biological function and inhibit cell division and proliferation.

If successful, this therapeutic approach may assist in treating metastatic diseases and may also help prevent the onset of the metastatic dissemination by targeting the pre-metastatic niches.

Key Words: p27 protein, recombinant proteins, liposomes.

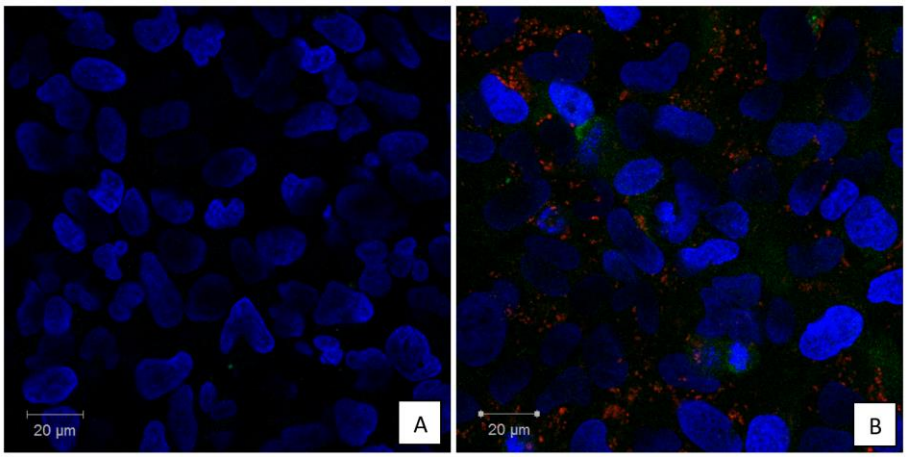

Figure 1: Localization of the liposomes and recombinant p27
The cell nucleus is marked in blue, the liposomes in red and the p27 in green
[A] U2OS cancer cells treated with empty liposomes
[B] U2OS cancer cells treated with p27 liposomes